Appl. Numer. Math. 208 (2025) 123–147

Contents lists available at ScienceDirect

Applied Numerical Mathematics

journal homepage: www.elsevier.com/locate/apnum

Research Paper

# A priori and a posteriori error estimates for efficient numerical schemes for coupled systems of linear and nonlinear singularly perturbed initial-value problems

Carmelo Clavero [a,*], Shashikant Kumar [b], Sunil Kumar [c]

[a] Department of Applied Mathematics and IUMA, University of Zaragoza, Zaragoza, Spain
[b] Department of Mathematics, Indian Institute of Technology Delhi, New Delhi, India
[c] Department of Mathematical Sciences, Indian Institute of Technology (BHU) Varanasi, Uttar Pradesh, India

ARTICLE INFO

*Keywords:*
Singular perturbation
A posteriori mesh
Computationally efficient
Splitting schemes
Monitor function
Nonlinear systems

ABSTRACT

This work considers the numerical approximation of linear and nonlinear singularly perturbed initial value coupled systems of first-order, for which the diffusion parameters at each equation of the system are distinct and also they can have a different order of magnitude. To do that, we use two efficient discretization methods, which combine the backward differences and an appropriate splitting by components. Both a priori and a posteriori error estimates are proved for the proposed discretization methods. The developed numerical methods are more computationally efficient than those classical methods used to solve the same type of coupled systems. Extensive numerical experiments strongly confirm in practice the theoretical results and corroborate the superior performance of the current approach compared with previous existing approaches.

## 1. Introduction

In the last years, the numerical treatment of singularly perturbed differential equations (SPDEs) has received much interest among applied mathematicians, because of its many applications in the frontier fields of science and engineering, such as fluid dynamics, quantum mechanics, chemical reactor theory, elasticity and porous gas electrodes theory. Mathematically, one or more of the highest-order derivative terms appearing in these problems are multiplied by a small positive parameter, popularly known as the perturbation parameter. When the parameter is very small, the solution exhibits thin layers, often adjacent to the boundaries of the domain of interest, where it varies rapidly. These regions are usually referred as boundary layers in fluid mechanics, edge layers in solid mechanics, skin layers in electrical applications and shock layers in solid mechanics. Suppose an analytic solution is sought in the form of an asymptotic expansion; in that case, different asymptotic expansions are needed in different parts of the domain, with no single expansion being uniformly valid everywhere [1]. Further, when attempting to approximate such solutions using well-known finite difference or finite element techniques on a uniform mesh, large oscillations may contaminate the numerical solution across the domain [2,3]. This situation worsens when dealing with coupled systems of two or more equations with distinct perturbation parameters, as their solutions contain overlapping and interacting layers, thus increasing the stiffness of the problem. Due to this complexity, developing appropriate numerical methods and conducting numerical analysis for the system of SPDEs becomes highly challenging. To this end, in this paper, we address an efficient numerical approximation of linear and nonlinear coupled systems

* Corresponding author.
*E-mail addresses:* clavero@unizar.es (C. Clavero), kashyapagyat@gmail.com (S. Kumar), skumar.iitd@gmail.com (S. Kumar).

https://doi.org/10.1016/j.apnum.2024.10.005
Received 27 June 2024; Received in revised form 3 October 2024; Accepted 7 October 2024

Available online 16 October 2024

of first-order SPDEs with prescribed initial conditions. Such systems are frequently exploited in the modeling of various real-life problems, such as the predator-prey model [4], the Alley model in population dynamics [5], dynamical systems [6], enzyme kinetics model in Biochemistry [7,8], the Lotka-Volterra population model or the host-parasitoid population dynamical model.

Several attempts have been made in the literature to approximate the solution of systems of first-order linear (see [9–13]) and nonlinear (see [7,8,14–20]) SPDEs. First, we present a review of the literature on works solving the system of first-order linear SPDEs. In [11], a system of two equations was considered in which the first equation is singularly perturbed, and the other equation is a non-perturbed differential equation. An almost first-order uniform convergence was shown on a piecewise uniform Shishkin mesh. In their analysis of a system of two SPDEs with distinct perturbation parameters, Rao and Kumar [12] achieved uniform convergence on a Shishkin mesh. The authors in [9,10] considered the linear system of SPDEs comprising an arbitrary number of equations, where in one case, all perturbation parameters are equal, while in another, they are distinct. They obtained an almost first-order convergence on a piecewise uniform Shishkin mesh. In [13], the system of an arbitrary number of SPDEs with distinct perturbation parameters was studied, and parameter uniform convergence was established on Shishkin and Bakhvalov meshes. Subsequently, the same problem was considered in [21], where they showed the convergence of a finite difference scheme on adaptive meshes. We now provide the literature review of works related to the system of first-order nonlinear SPDEs. In [14], the nonlinear system of two equations was considered in which the first equation is first-order nonlinear SPDE while the other equation is a second-order non-perturbed differential equation. Using a finite difference scheme, a first-order convergence was achieved on a Shishkin mesh. For a system of two nonlinear SPDEs, a first-order convergent numerical method on a Shishkin mesh was given in [7]. Moreover, authors in [17] developed a general error analysis framework on both Shishkin and Bakhvalov meshes. In [18,19], uniformly convergent methods based on adaptive meshes were developed.

Observe that the authors in [7,9–17] used a priori meshes, such as Shishkin and Bakhvalov meshes, to resolve the layer phenomena. Such meshes appear to be an appealing choice due to their ease of generation, lower computational cost and ability to handle a wide range of SPDEs. However, the construction of a priori meshes is highly dependent on a priori knowledge of the behavior of the exact solution and its derivatives. Typically, the information needed about the solution is not always available in advance. It is well known that a posteriori mesh (or adaptive moving mesh) is a better alternative than a priori meshes because, unlike a priori meshes, it does not require a priori knowledge of the behavior of the exact solution and their derivatives. In general, such meshes are generated using a suitable monitor function and the equidistribution principle [22,23]. A critical aspect of such methods is selecting an appropriate monitor function. Some papers considered the arc-length monitor functions [21] and some considered a suitable monitor function based on the bounds of the a posteriori error analysis [20].

It is worth mentioning here that all of the above papers require a significant amount of computing time (or computational cost) to solve linear or nonlinear systems with an arbitrary number of equations because the components of the discrete solution are coupled. Numerical analysts are often interested in developing numerical schemes that provide good approximations with a low computational cost [24–27]. To the best of our knowledge, no researcher has attempted to reduce the computational cost for approximating first-order linear and nonlinear coupled systems of SPDEs. Further, it is important to note that the previous works on nonlinear systems of first-order SPDEs are restricted to two equations. Thus, the main contribution of the present paper is as follows:

- To develop efficient discretization methods for solving linear and nonlinear coupled systems of first-order singularly perturbed initial value problems with distinct perturbation parameters.
- To derive a priori and a posteriori error estimates for the proposed efficient discretization methods.
- To address nonlinear coupled systems of first-order SPDEs with an arbitrary number of equations.

The paper is organized into two major sections. Section 2 addresses a linear coupled system and its stability. The discretization of the linear system is given in Subsection 2.1. Afterwards, a priori and a posteriori error analysis is given in the Subsections 2.2 & 2.3, respectively. In a similar fashion, we analyze a nonlinear coupled system in Section 3. In section 4 we perform some numerical experiments to validate in practice the theoretical results. Finally, we finish this work with a short section of conclusions.

**Notations:** Throughout the paper, we use $C$ to denote a generic positive constant independent of all the perturbation and discretization parameters. Define $\boldsymbol{v} \leq \boldsymbol{w}$ if $v_k \leq w_k$, $k = 1, \ldots, \ell$, and $|v| = \left(|v_1|, \ldots, |v_\ell|\right)^T$. For any function $g \in C(\overline{\Omega})$, define $g_j = g(x_j)$; if $\boldsymbol{g} \in C(\overline{\Omega})^\ell$ then $\boldsymbol{g}_j = \boldsymbol{g}(x_j) = \left(g_{1,j}, \ldots, g_{\ell,j}\right)^T$. The continuous maximum norm is denoted by $\|g\|_\infty = \max\limits_{x \in \overline{\Omega}} |g(x)|$ and $\|\boldsymbol{g}\|_\infty = \max\limits_{j=1,\ldots,\ell} \|g_j\|_\infty$. The analogous discrete maximum norm on the mesh $\overline{\Omega}^N$ is denoted by $\|\cdot\|_{\overline{\Omega}^N}$.

## 2. A coupled system of linear SPIVPs

We consider the following class of SPDEs, which consists of a system of $\ell$ first-order linear differential equations of the form

$$\begin{cases} \boldsymbol{\mathcal{L}}\boldsymbol{y}(x) := \mathcal{E}\boldsymbol{y}'(x) + \mathcal{A}(x)\boldsymbol{y}(x) = \boldsymbol{g}(x), \qquad x \in \Omega = (0,1], & \text{(a)} \\ \boldsymbol{y}(0) = \boldsymbol{\gamma}, & \text{(b)} \end{cases} \tag{2.1}$$

where the solution $\boldsymbol{y} = \left(y_1, \ldots, y_\ell\right)^T$, the right hand side function $\boldsymbol{g} = \left(g_1, \ldots, g_\ell\right)^T$ and the initial condition $\boldsymbol{\gamma} = \left(\gamma_1, \ldots, \gamma_\ell\right)^T$ are column vectors; $\mathcal{E} = \operatorname{diag}(\epsilon_1, \ldots, \epsilon_\ell)$ is a diagonal matrix with small distinct perturbation parameters $0 < \epsilon_i \leq \epsilon_j \ll 1$ for $1 \leq i < j \leq \ell$, $\mathcal{A}(x) = \left(a_{ij}(x)\right)_{1 \leq i,j \leq \ell}$, and $\boldsymbol{\mathcal{L}}\boldsymbol{y} = \left(\mathcal{L}_1\boldsymbol{y}, \ldots, \mathcal{L}_\ell\boldsymbol{y}\right)^T$ with

$$\mathcal{L}_i \boldsymbol{y}(x) := \epsilon_i y_i'(x) + \sum_{j=1}^{\ell} a_{ij}(x) y_j(x) = g_i(x), \ 1 \le i \le \ell. \tag{2.2}$$

Furthermore, we assume that the elements of the matrix $\mathcal{A}$ satisfy the following conditions for all $x \in \overline{\Omega} = \Omega \cup \{0\}$ :

$$\begin{cases} a_{ii}(x) > 0, & i = 1, \dots, \ell, \quad \text{(a)} \\ \sum_{\substack{m=1 \\ m \neq i}}^{\ell} \| \frac{a_{im}}{a_{ii}} \|_\infty < \zeta < 1, & i = 1, \dots, \ell, \quad \text{(b)} \end{cases} \tag{2.3}$$

for an arbitrary number $\zeta$. It is well established in [13] that the system (2.1a)–(2.1b) has a unique solution $\boldsymbol{y} \in C^2(\overline{\Omega})^\ell$ under the above assumptions. Note that, from the positivity conditions (2.3a)–(2.3b), in general, it does not follow that the differential operator $\boldsymbol{\mathcal{L}}$ satisfies a maximum principle; still it is maximum norm stable, as given below.

**Lemma 2.1.** *Under the assumptions (2.3a)–(2.3b), the continuous solution vector $\boldsymbol{y}$ of (2.1a)–(2.1b) satisfies*

$$\|y_i\|_\infty \le \sum_{m=1}^{\ell} (\boldsymbol{\Lambda}^{-1})_{im} \max \left\{ \| \frac{g_m}{a_{mm}} \|_\infty, |\gamma_m| \right\}, \quad i = 1, \dots, \ell, \tag{2.4}$$

*where $\boldsymbol{\Lambda} = \left( \eta_{ij} \right)_{1 \le i,j \le \ell}$ is a $\ell \times \ell$ matrix such that $\eta_{ii} = 1$ and $\eta_{ij} = -\| \frac{a_{ij}}{a_{ii}} \|_\infty$ for $i \neq j$.*

**Proof.** The proof of this lemma follows from [13, Lemma 2.2]. □

Using the above Lemma, we can establish the following corollary, which is crucial for the posterior analysis of our numerical schemes.

**Corollary 2.1.** *Consider any two continuous vector functions $\boldsymbol{u}$ and $\boldsymbol{v}$ satisfying*

$$\boldsymbol{\mathcal{L}u}(x) - \boldsymbol{\mathcal{L}v}(x) = \boldsymbol{\mathcal{G}}(x), \quad \boldsymbol{u}(0) = \boldsymbol{v}(0),$$

*where $\boldsymbol{\mathcal{G}}$ is a bounded piecewise continuous vector function. Then, it holds*

$$\|\boldsymbol{u} - \boldsymbol{v}\|_\infty \le C_1 \|\boldsymbol{\mathcal{L}u} - \boldsymbol{\mathcal{L}v}\|_\infty. \tag{2.5}$$

**Proof.** For simplicity, we denote $\boldsymbol{\psi} = \boldsymbol{u} - \boldsymbol{v}$. Observe that $\boldsymbol{\mathcal{L}\psi}(x) = \boldsymbol{\mathcal{L}}(\boldsymbol{u}(x) - \boldsymbol{v}(x)) = \boldsymbol{\mathcal{L}u}(x) - \boldsymbol{\mathcal{L}v}(x)$. Consequently, we have

$$\begin{cases} \boldsymbol{\mathcal{L}\psi}(x) := \mathcal{E}\boldsymbol{\psi}'(x) + \mathcal{A}(x)\boldsymbol{\psi}(x) = \boldsymbol{\mathcal{G}}(x), & x \in \Omega = (0, 1], \\ \boldsymbol{\psi}(0) = \boldsymbol{0}. \end{cases}$$

Clearly, the above system of equations is of the form of (2.1a)–(2.1b). Therefore, using Lemma 2.1, we get

$$\|\psi_i\|_\infty = \|u_i - v_i\|_\infty \le \sum_{m=1}^{\ell} \left( \boldsymbol{\Lambda}^{-1} \right)_{im} \max \left\{ \| \frac{\mathcal{G}_m}{a_{mm}} \|_\infty, |0| \right\}, \quad i = 1, \dots, \ell.$$

Hence, using vector notation, the above inequality gives the required estimate (2.5). □

Next, we provide the derivative bounds of the continuous solution, which will be helpful to obtain the a priori error estimates in later subsections.

**Lemma 2.2.** *Let $\boldsymbol{y}_r$ and $\boldsymbol{y}_b$ denote the regular and singular components of the continuous solution $\boldsymbol{y}$. Then, $\boldsymbol{y}_r$ and $\boldsymbol{y}_b$ satisfy the following derivative estimates*

$$\begin{cases} \|y_{r,i}^{(s)}\|_\infty \le C, \ \ s = 0, 1, \qquad \epsilon_i \|y_{r,i}^{(2)}\|_\infty \le C, & \text{(a)} \\ |y_{b,i}^{(s)}(x)| \le C \sum_{m=i}^{\ell} \epsilon_m^{-s} \exp\left( -\frac{\alpha x}{\epsilon_m} \right), \ \ s = 0, 1, & \text{(b)} \\ \epsilon_i |y_{b,i}^{(2)}(x)| \le C \sum_{m=1}^{\ell} \epsilon_m^{-1} \exp\left( -\frac{\alpha x}{\epsilon_m} \right), & \text{(c)} \end{cases} \tag{2.6}$$

*for $i = 1, \dots, \ell$ and $\alpha := (1 - \zeta) \min\limits_{m=1,\dots,\ell} \min\limits_{x \in \overline{\Omega}} a_{mm}(x)$.*

**Proof.** Consider the decomposition of continuous solution as $\boldsymbol{y} = \boldsymbol{y}_r + \boldsymbol{y}_b$, where the regular component $\boldsymbol{y}_r$ and the singular component $\boldsymbol{y}_b$ satisfy the following problems

$$\begin{cases} \boldsymbol{\mathcal{L}}\boldsymbol{y}_r = \boldsymbol{g} \text{ in } \Omega, & \boldsymbol{y}_r(0) = \mathcal{A}(0)^{-1}\boldsymbol{g}(0), \quad \text{(a)} \\ \boldsymbol{\mathcal{L}}\boldsymbol{y}_b = \boldsymbol{0} \text{ in } \Omega, & \boldsymbol{y}_b(0) = \boldsymbol{y}(0) - \boldsymbol{y}_r(0). \quad \text{(b)} \end{cases} \tag{2.7}$$

From Lemma 2.1, it follows that $\|\boldsymbol{y}_r\|_\infty \le C$. From (2.7a), we observe that $\epsilon_i y'_{r,i}(0) = 0,\ i = 1, \dots, \ell$, and therefore, it holds

$$\boldsymbol{\mathcal{L}}\boldsymbol{y}'_r = \boldsymbol{g}' - \mathcal{A}'\boldsymbol{y}_r \text{ in } \Omega, \quad \boldsymbol{y}'_r(0) = \boldsymbol{0}. \tag{2.8}$$

After applying Lemma 2.1 and the bound on $\boldsymbol{y}_r$ to (2.8), we get $\|\boldsymbol{y}'_r\|_\infty \le C$. Finally, making use of (2.8) along with bounds on $\boldsymbol{y}_r$ and $\boldsymbol{y}'_r$, we get $\epsilon_i \|y^{(2)}_{r,i}\|_\infty \le C$, for $i = 1, \dots, \ell$.

Next, the bounds on the singular part $\boldsymbol{y}_b$ can be derived by imitating the arguments presented in [13]. □

### 2.1. The discrete problem

We consider an arbitrary nonuniform grid $\overline{\Omega}^N := \{x_k \mid 0 = x_0 < x_1 < \cdots < x_N = 1\}$ that discretizes the continuous domain $\overline{\Omega}$ into $N+1$ grid points with nonuniform step-sizes $h_k = x_k - x_{k-1}$ for all $1 \le k \le N$. We denote the set of interior grid points with $\Omega^N = \overline{\Omega}^N \setminus \{0\}$. We propose the following splitting schemes based discretization for the continuous problem (2.1a)–(2.1b) on $\overline{\Omega}^N$:

$$\begin{cases} \boldsymbol{\mathcal{L}}^N \boldsymbol{Y}(x_k) := \mathcal{E}D^-\boldsymbol{Y}(x_k) + \mathcal{P}(x_k)\boldsymbol{Y}(x_k) - \mathcal{Q}(x_k)\boldsymbol{Y}(x_{k-1}) = \boldsymbol{g}(x_k), \quad x_k \in \Omega^N, & \text{(a)} \\ \boldsymbol{Y}_0 = \boldsymbol{\gamma}, & \text{(b)} \end{cases} \tag{2.9}$$

where $\boldsymbol{Y}$ is the approximation of $\boldsymbol{y}$, $\boldsymbol{\mathcal{L}}^N = \left(\mathcal{L}^N_1, \dots, \mathcal{L}^N_\ell\right)^T$, $D^-$ is the backward difference operator defined as

$$D^-\boldsymbol{W}(x_k) := \frac{\boldsymbol{W}(x_k) - \boldsymbol{W}(x_{k-1})}{h_k}, \quad 1 \le k \le N, \tag{2.10}$$

for any mesh vector function $\boldsymbol{W}$, and $\mathcal{A}(x_k) = \mathcal{P}(x_k) - \mathcal{Q}(x_k)$.

Here, the matrix $\mathcal{P}$ has three possibilities. The above discretization reduces to the backward Euler scheme for $\mathcal{A} = \mathcal{P}$ which is considered in [13], where only a priori error analysis of the scheme was given. The rest two other possibilities can be chosen from the set $\mathcal{P} = \left\{\mathcal{P}_{\text{diag}}, \mathcal{P}_{\text{ltr}}\right\}$, where

$$\mathcal{P}_{\text{diag}} = \left(a_{ij}\right) \text{ with } a_{ij} = \begin{cases} a_{ii}, & \text{for } i = j, \\ 0, & \text{for } i \ne j, \end{cases} \qquad \mathcal{P}_{\text{ltr}} = \left(a_{ij}\right) \text{ with } a_{ij} = \begin{cases} a_{ij}, & \text{for } i \ge j, \\ 0, & \text{for } i < j. \end{cases}$$

Consequently, the matrix $\mathcal{Q}$ can be computed by subtracting $\mathcal{P}$ to $\mathcal{A}$. Further, we rewrite the discretization scheme (2.9a)–(2.9b) corresponding to $\mathcal{P}_{\text{diag}}$ and $\mathcal{P}_{\text{ltr}}$ as follows.

**Case 1:** If $\mathcal{P} = \mathcal{P}_{\text{diag}}$, then

$$\mathcal{L}^N_i \boldsymbol{Y}(x_k) := \epsilon_i D^- Y_i(x_k) + a_{ii}(x_k)Y_i(x_k) + \sum_{\substack{m=1 \\ m \ne i}}^{\ell} a_{im}(x_k)Y_m(x_{k-1}) = g_i(x_k), \quad i = 1, \dots, \ell. \tag{2.11}$$

**Case 2:** Similarly, if $\mathcal{P} = \mathcal{P}_{\text{ltr}}$, then

$$\mathcal{L}^N_i \boldsymbol{Y}(x_k) := \epsilon_i D^- Y_i(x_k) + \sum_{m=1}^{i} a_{im}(x_k)Y_m(x_k) + \sum_{m=i+1}^{\ell} a_{im}(x_k)Y_m(x_{k-1}) = g_i(x_k), \quad i = 1, \dots, \ell. \tag{2.12}$$

To ease the calculations in subsequent subsections, we provide the following general form of the above cases

$$\begin{aligned} \mathcal{L}^N_i \boldsymbol{Y}(x_k) &:= \epsilon_i D^- Y_i(x_k) + a_{ii}(x_k)Y_i(x_k) + \sum_{m=1}^{i-1} a_{im}(x_k)Y_m(x_{k-\sigma}) + \sum_{m=i+1}^{\ell} a_{im}(x_k)Y_m(x_{k-1}) \\ &= g_i(x_k), \quad i = 1, \dots, \ell, \end{aligned} \tag{2.13}$$

$$Y_i(x_0) = \gamma_i, \tag{2.14}$$

where $\sigma$ can be 0 or 1; when $\sigma = 1$, then the above scheme corresponds to Case 1 ($\mathcal{P} = \mathcal{P}_{\text{diag}}$), and for $\sigma = 0$, it corresponds to Case 2 ($\mathcal{P} = \mathcal{P}_{\text{ltr}}$).

### 2.2. A priori error analysis

In this subsection, we present the a priori error analysis of the discrete scheme (2.9a)–(2.9b). Before we proceed further, we first provide the stability estimate of the discrete scheme defined in the previous subsection. This requires the following result.

**Lemma 2.3.** *For $\epsilon > 0$, $c(x) > 0$ and $\boldsymbol{\Phi} \in \mathbb{R}^{N+1}$, if $\epsilon D^- \boldsymbol{\Phi}(x_k) + c(x_k)\boldsymbol{\Phi}(x_k) = g(x_k)$, $k = 1, \ldots, N$, the following result holds*

$$\|\boldsymbol{\Phi}\|_{\overline{\Omega}^N} \leq \max\left\{ \|\frac{g}{c}\|_{\Omega^N}, |\boldsymbol{\Phi}_0| \right\}. \tag{2.15}$$

**Proof.** The proof of this lemma can be readily proven using the arguments similar to [13, Lemma 2.1]. □

**Lemma 2.4** *(Stability estimate). Under the assumptions on coupling matrix $\mathcal{A}$ given in (2.3a)–(2.3b), the discrete solution $\boldsymbol{Y}$ of (2.9a)–(2.9b) satisfies the following stability estimate $\forall\ i = 1, \ldots, \ell$,*

$$\|Y_i\|_{\overline{\Omega}^N} \leq \sum_{m=1}^{\ell} (\boldsymbol{\Lambda}^{-1})_{im} \max\left\{ \|\frac{g_m}{a_{mm}}\|_{\Omega^N}, |\gamma_m| \right\}. \tag{2.16}$$

**Proof.** Let us decompose the discrete solution as $\boldsymbol{Y} = \boldsymbol{U} + \boldsymbol{V}$, where the $i^{\text{th}}$-component of $\boldsymbol{U}$ and $\boldsymbol{V}$ are the solutions of the discrete problems

$$\epsilon_i D^- U_i(x_k) + a_{ii}(x_k) U_i(x_k) = g_i(x_k), \quad U_i(x_0) = \gamma_i,$$

and

$$\epsilon_i D^- V_i(x_k) + a_{ii}(x_k) V_i(x_k) = -\sum_{m=1}^{i-1} a_{im}(x_k) Y_m(x_{k-\sigma}) - \sum_{m=i+1}^{\ell} a_{im}(x_k) Y_m(x_{k-1}), \quad V_i(x_0) = 0,$$

respectively, where we have used (2.13)-(2.14).

By virtue of Lemma 2.3, we can obtain

$$\|U_i\|_{\overline{\Omega}^N} \leq \max\left\{ \|\frac{g_i}{a_{ii}}\|_{\Omega^N}, |\gamma_i| \right\} \quad \text{and} \quad \|V_i\|_{\overline{\Omega}^N} \leq \sum_{\substack{m=1 \\ m \neq i}}^{\ell} \|\frac{a_{im}}{a_{ii}}\|_{\Omega^N} \|Y_m\|_{\overline{\Omega}^N}.$$

Using the triangle inequality, we get

$$\|Y_i\|_{\overline{\Omega}^N} \leq \|U_i\|_{\overline{\Omega}^N} + \|V_i\|_{\overline{\Omega}^N} \leq \|U_i\|_{\overline{\Omega}^N} + \sum_{\substack{m=1 \\ m \neq i}}^{\ell} \|\frac{a_{im}}{a_{ii}}\|_{\Omega^N} \|Y_m\|_{\overline{\Omega}^N}.$$

Consequently, it holds

$$\|Y_i\|_{\overline{\Omega}^N} - \sum_{\substack{m=1 \\ m \neq i}}^{\ell} \|\frac{a_{im}}{a_{ii}}\|_{\Omega^N} \|Y_m\|_{\overline{\Omega}^N} \leq \max\left\{ \|\frac{g_i}{a_{ii}}\|_{\Omega^N}, |\gamma_i| \right\}, \quad i = 1, 2, \ldots, \ell.$$

Finally, using the inverse monotonicity of $\boldsymbol{\Lambda}$, we obtain the required result (2.16). □

**Theorem 2.1.** *If $\boldsymbol{y}$ is the solution of (2.1a)–(2.1b) and $\boldsymbol{Y}$ is the approximate solution of (2.9a)–(2.9b) obtained on an arbitrary nonuniform mesh $\overline{\Omega}^N$, then we have the following a priori error estimate*

$$\|\boldsymbol{y} - \boldsymbol{Y}\|_{\overline{\Omega}^N} \leq C\vartheta(\Omega^N), \tag{2.17}$$

*where* $\vartheta(\Omega^N) := \max\limits_{1 \leq k \leq N} \int\limits_{x_{k-1}}^{x_k} \left( 1 + \sum\limits_{m=1}^{\ell} \epsilon_m^{-1} \exp\left( -\frac{\alpha s}{\epsilon_m} \right) \right) ds.$

**Proof.** Let us consider an error vector for the discrete scheme (2.13)–(2.14) as $\boldsymbol{\xi} = \boldsymbol{y} - \boldsymbol{Y}$, where $\xi_i(x_k) = y_i(x_k) - Y_i(x_k)$, $1 \leq i \leq \ell$, $1 \leq k \leq N$. Now we introduce a new operator defined by

$$\widehat{\mathcal{L}}_i^N \boldsymbol{Y}(x_k) := \epsilon_i D^- Y_i(x_k) + a_{ii}(x_k) Y_i(x_k),$$

and we divide the error into two parts $\boldsymbol{\xi} = \boldsymbol{\xi_1} + \boldsymbol{\xi_2}$, such that $\forall\ 1 \leq i \leq \ell$, it holds

$$\begin{cases} \widehat{\mathcal{L}}_i^N \boldsymbol{\xi_1}(x_k) = \mathcal{L}_i^N \boldsymbol{\xi}(x_k), \qquad \xi_{1,i}(0) = 0, & \text{(a)} \\ \widehat{\mathcal{L}}_i^N \boldsymbol{\xi_2}(x_k) = -\sum_{m=1}^{i-1} a_{im}(x_k) \xi_m(x_{k-\sigma}) - \sum_{m=i+1}^{\ell} a_{im}(x_k) \xi_m(x_{k-1}), \qquad \xi_{2,i}(0) = 0, & \text{(b)} \end{cases} \tag{2.18}$$

for all $1 \leq k \leq N$.

The triangle inequality together with Lemma 2.4 yields

$$\|\xi_i\|_{\overline{\Omega}^N} \le \|\xi_{1,i}\|_{\overline{\Omega}^N} + \|\xi_{2,i}\|_{\overline{\Omega}^N} \le \|\xi_{1,i}\|_{\overline{\Omega}^N} + \sum_{\substack{m=1\\ m\neq i}}^{\ell} \|\frac{a_{im}}{a_{ii}}\|_{\Omega^N} \|\xi_m\|_{\overline{\Omega}^N}.$$

Hence, we get

$$\|\xi_i\|_{\overline{\Omega}^N} - \sum_{\substack{m=1\\ m\neq i}}^{\ell} \|\frac{a_{im}}{a_{ii}}\|_{\Omega^N} \|\xi_m\|_{\overline{\Omega}^N} \le \|\xi_{1,i}\|_{\overline{\Omega}^N}, \quad 1 \le i \le \ell.$$

Now, appealing to inverse monotonicity of $\mathbf{\Lambda}^{-1}$, it follows

$$\|\xi_i\|_{\overline{\Omega}^N} = \|y_i - Y_i\|_{\overline{\Omega}^N} \le C\|\xi_{1,i}\|_{\overline{\Omega}^N}, \quad i = 1, \ldots, \ell. \tag{2.19}$$

We observe that the components of $\boldsymbol{\xi_1}$ are the solutions of the problems

$$\widehat{\mathcal{L}}_i^N \boldsymbol{\xi_1}(x_k) := \epsilon_i \left(D^- y_i(x) - \frac{d}{dx} y_i(x)\right)\Big|_{x=x_k} + \sum_{m=1}^{i-1} a_{im}(x_k)\Big(y_m(x_{k-\sigma}) - y_m(x_k)\Big)$$
$$+ \sum_{m=i+1}^{\ell} a_{im}(x_k)\Big(y_m(x_{k-1}) - y_m(x_k)\Big), \quad 1 \le k \le N,$$

with $\xi_{1,i}(0) = 0 \ \forall\ 1 \le i \le \ell$, since it satisfies (2.18a) and also

$$\widehat{\mathcal{L}}_i^N \boldsymbol{\xi_1}(x_k) = \mathcal{L}_i^N \boldsymbol{\xi}(x_k) = \mathcal{L}_i^N \boldsymbol{y}(x_k) - \mathcal{L}_i^N \boldsymbol{Y}(x_k) = (\mathcal{L}_i^N - \mathcal{L}_i)\boldsymbol{y}(x_k)$$
$$= \epsilon_i \left(D^- y_i(x) - \frac{d}{dx} y_i(x)\right)\Big|_{x=x_k} + \sum_{m=1}^{i-1} a_{im}(x_k)\Big(y_m(x_{k-\sigma}) - y_m(x_k)\Big)$$
$$+ \sum_{m=i+1}^{\ell} a_{im}(x_k)\Big(y_m(x_{k-1}) - y_m(x_k)\Big).$$

Therefore, it follows

$$|\widehat{\mathcal{L}}_i^N \boldsymbol{\xi_1}(x_k)| \le \epsilon_i |\left(D^- y_i(x) - \frac{d}{dx} y_i(x)\right)\Big|_{x=x_k}| + |\sum_{m=1}^{i-1} a_{im}(x_k) \int_{x_{k-\sigma}}^{x_k} y_m'(s)\, ds|$$
$$+ |\sum_{m=i+1}^{\ell} a_{im}(x_k) \int_{x_{k-1}}^{x_k} y_m'(s)\, ds|$$
$$\le \epsilon_i \int_{x_{k-1}}^{x_k} |y_i''(s)|\, ds + C \int_{x_{k-\sigma}}^{x_k} \sum_{m=1}^{i-1} |y_m'(s)|\, ds + C \int_{x_{k-1}}^{x_k} \sum_{m=i+1}^{\ell} |y_m'(s)|\, ds$$
$$\le C \int_{x_{k-1}}^{x_k} \left(1 + \sum_{m=1}^{\ell} \epsilon_m^{-1} \exp\left(-\frac{\alpha s}{\epsilon_m}\right)\right) ds,$$

where we have used the Taylor expansion with the integral form of remainder and we made use of derivative bounds of $\boldsymbol{y}$ given in Lemma 2.2. Further, a direct application of Lemma 2.3 gives

$$\|\xi_{1,i}\|_{\overline{\Omega}^N} \le C \max_{1\le k\le N} \int_{x_{k-1}}^{x_k} \left(1 + \sum_{m=1}^{\ell} \epsilon_m^{-1} \exp\left(-\frac{\alpha s}{\epsilon_m}\right)\right) ds, \quad i = 1, \ldots, \ell \tag{2.20}$$

Finally, plugging the bounds of (2.20) in (2.19) gives the required estimate (2.17). □

The general convergence result of Theorem 2.1 provides the means to guarantee the uniform convergence of discrete scheme (2.9a)–(2.9b) on a variety of special layer-adapted meshes; nevertheless, here we confine ourselves to Shishkin and Bakhvalov meshes.

**Shishkin meshes:** These meshes are special piecewise uniform meshes that resolve the layer phenomena of the problem. To construct them, we define the transition parameters as follows (see [28]):

$$\tau_0 = 0, \quad \tau_m = \min\left\{\frac{m\tau_{m+1}}{m+1}, \frac{\mu\epsilon_m}{\alpha}\ln N\right\}, \quad m = \ell, \ldots, 1, \quad \text{and } \tau_{\ell+1} = 1, \tag{2.21}$$

where $\mu$ is a positive constant to be defined later on.

**Corollary 2.2.** *Let $\boldsymbol{y}$ denote the solution of (2.1a)–(2.1b) and $\boldsymbol{Y}$ represent the approximate solution of (2.9a)–(2.9b) obtained on Shishkin mesh, as defined in (2.21). Then, the following estimate holds*

$$\|\boldsymbol{y} - \boldsymbol{Y}\|_{\bar{\Omega}^N} \leq CN^{-1}\ln N, \quad \text{if } \mu \geq 1.$$

**Proof.** Assuming that $N$ is divisible by $\ell+1$, the transition parameters partition the interval $[0,1]$ as $[0,\tau_1]\cup[\tau_1,\tau_2]\cdots\cup[\tau_\ell,1]$ with $1+N/(\ell+1)$ equidistant mesh points on each subinterval. For what follows, we assume that $\tau_m = \frac{\mu\epsilon_m}{\alpha}\ln N, m = \ell, \ldots, 1$, as otherwise $N^{-1}$ is exponentially small compared to $\epsilon_i, i = 1, \ldots, \ell$ and the analysis can be done in a classical way. It is straightforward to deduce that it holds

$$\int_{x_{k-1}}^{x_k}\left(1 + \sum_{m=1}^{\ell}\epsilon_m^{-1}\exp\left(-\frac{\alpha s}{\epsilon_m}\right)\right)ds \leq h_k + \frac{1}{\alpha}\sum_{m=1}^{\ell}|\exp\left(-\frac{\alpha x_{k-1}}{\epsilon_m}\right) - \exp\left(-\frac{\alpha x_k}{\epsilon_m}\right)|. \tag{2.22}$$

Now, we consider the region $[0,\tau_1]$. Using the mean value theorem, there exists $\nu \in (x_{k-1}, x_k)$, such that

$$\begin{aligned}\int_{x_{k-1}}^{x_k}\left(1 + \sum_{m=1}^{\ell}\epsilon_m^{-1}\exp\left(-\frac{\alpha s}{\epsilon_m}\right)\right)ds &\leq h_k\left\{1 + \sum_{m=1}^{\ell}\epsilon_m^{-1}\exp\left(-\frac{\alpha\nu}{\epsilon_m}\right)\right\}\\ &\leq CN^{-1}\ln N,\end{aligned}$$

where we have used that $h_k \leq \epsilon_1 N^{-1}\ln N$ holds.

Next, we consider the region $[\tau_\ell, 1]$. The condition $0 < \epsilon_i \leq \epsilon_j \ll 1$ for $1 \leq i < j \leq \ell$, implies that $\exp\left(-\frac{\alpha x_{k-1}}{\epsilon_i}\right) \leq \exp\left(-\frac{\alpha x_{k-1}}{\epsilon_\ell}\right)$ and $\exp\left(-\frac{\alpha x_k}{\epsilon_i}\right) \leq \exp\left(-\frac{\alpha x_k}{\epsilon_\ell}\right)$ for $i = 1, \ldots, \ell$. Further, $x_{k-1} \leq x_k$ implies that $\exp\left(-\frac{\alpha x_k}{\epsilon_\ell}\right) \leq \exp\left(-\frac{\alpha x_{k-1}}{\epsilon_\ell}\right)$. Hence, from (2.22) we can obtain

$$\begin{aligned}\int_{x_{k-1}}^{x_k}\left(1 + \sum_{m=1}^{\ell}\epsilon_m^{-1}\exp\left(-\frac{\alpha s}{\epsilon_m}\right)\right)ds &\leq h_k + \frac{C}{\alpha}\exp\left(-\frac{\alpha x_{k-1}}{\epsilon_\ell}\right)\\ &\leq C\left(N^{-1}\ln N + N^{-\mu}\right),\end{aligned}$$

where we have used the definition of $\tau_\ell$. Finally, we consider the region $[\tau_i, \tau_{i+1}]$ for $i = 1, 2, \ldots, \ell-1$. Using (2.22), we have

$$\begin{aligned}&\int_{x_{k-1}}^{x_k}\left(1 + \sum_{m=1}^{\ell}\epsilon_m^{-1}\exp\left(-\frac{\alpha s}{\epsilon_m}\right)\right)ds\\ &\leq h_k + \frac{1}{\alpha}\sum_{m=1}^{i}|\exp\left(-\frac{\alpha x_{k-1}}{\epsilon_m}\right) - \exp\left(-\frac{\alpha x_k}{\epsilon_m}\right)| + \frac{1}{\alpha}\sum_{m=i+1}^{\ell}|\exp\left(-\frac{\alpha x_{k-1}}{\epsilon_m}\right) - \exp\left(-\frac{\alpha x_k}{\epsilon_m}\right)|\\ &\leq h_k + \frac{C}{\alpha}\exp\left(-\frac{\alpha x_{k-1}}{\epsilon_i}\right) + h_k\sum_{m=i+1}^{\ell}\epsilon_m^{-1}\exp\left(-\frac{\alpha\nu}{\epsilon_m}\right)\\ &\leq C\left(N^{-1}\ln N + N^{-\mu}\right),\end{aligned} \tag{2.23}$$

where we have used the previous arguments and also that it holds $h_k \leq C\epsilon_{i+1}N^{-1}\ln N$.

Finally, combining the estimates obtained for all regions, on this mesh, we obtain

$$\vartheta(\Omega^N) \leq C(N^{-\mu} + N^{-1}\ln N).$$

Consequently, Theorem 2.1 gives

$$\|\boldsymbol{y} - \boldsymbol{Y}\|_{\bar{\Omega}^N} \leq CN^{-1}\ln N, \quad \text{if } \mu \geq 1. \quad \square$$

**Bakhvalov meshes:** These meshes are graded in nature and superior to the Shishkin meshes. To discretize the problem, we construct the Bakhvalov meshes using the idea of the equidistribution principle for the monitor function (see [28])

$$B_M(x) := \max\left\{1, \frac{\varsigma_1}{\epsilon_1}e^{-\alpha x/\mu\epsilon_1}, \ldots, \frac{\varsigma_\ell}{\epsilon_\ell}e^{-\alpha x/\mu\epsilon_\ell}\right\}, \tag{2.24}$$

where $\varsigma_i > 0,\ i = 1, \ldots, \ell$ is a user-chosen constant.

**Corollary 2.3.** *Let $\boldsymbol{y}$ denote the solution of (2.1a)–(2.1b) and $\boldsymbol{Y}$ represent the approximate solution of (2.9a)–(2.9b) obtained on Bakhvalov mesh, as defined in (2.24). Then, the following estimate holds*

$$\|\boldsymbol{y} - \boldsymbol{Y}\|_{\overline{\Omega}^N} \leq CN^{-1}, \quad \text{if } \mu \geq 1,$$

**Proof.** From the equidistribution principle, it follows that

$$\int_{x_{k-1}}^{x_k} B_M(x)\,dx = \frac{1}{N}\int_0^1 B_M(x)\,dx, \quad k = 1, \ldots, N.$$

Clearly, $\int_0^1 B_M(x)\,dx \leq C$. Further, for $\mu \geq 1$ and arbitrary $\varsigma_i > 0,\ i = 1, \ldots, \ell$, there exists a constant $C$ such that

$$1 + \sum_{m=1}^{\ell} \epsilon_m^{-1} \exp\left(-\frac{\alpha x}{\epsilon_m}\right) \leq C \max\left\{1, \frac{\varsigma_1}{\epsilon_1} e^{-\alpha x/\mu\epsilon_1}, \ldots, \frac{\varsigma_\ell}{\epsilon_\ell} e^{-\alpha x/\mu\epsilon_\ell}\right\} = C B_M(x).$$

Hence, we have

$$\int_{x_{k-1}}^{x_k} \left(1 + \sum_{m=1}^{\ell} \epsilon_m^{-1} \exp\left(-\frac{\alpha x}{\epsilon_m}\right)\right) dx \leq C \int_{x_{k-1}}^{x_k} B_M(x)\,dx,$$

and therefore it holds

$$\vartheta(\Omega^N) \leq \frac{C}{N}\int_0^1 B_M(x)\,dx \leq CN^{-1}.$$

Thereby, Theorem 2.1 gives

$$\|\boldsymbol{y} - \boldsymbol{Y}\|_{\overline{\Omega}^N} \leq CN^{-1}, \quad \text{if } \mu \geq 1,$$

which proves the first order of uniform convergence when the Bakhvalov mesh is used. □

### 2.3. A posteriori error analysis

We now give the a posteriori error analysis corresponding to the linear discrete problem (2.9a)–(2.9b). For this, we assume a piecewise linear interpolant vector $\widetilde{\boldsymbol{Y}}(x)$ corresponding to the discrete solution vector $\boldsymbol{Y}(x_k)\,\forall\, k = 1, \ldots, N$. Clearly, $\widetilde{\boldsymbol{Y}}(x)$ is continuous on $\overline{\Omega}$, linear on each sub-intervals $[x_{k-1}, x_k]$ and defined by

$$\widetilde{\boldsymbol{Y}}(x) = \boldsymbol{Y}(x_k) + (x - x_k)D^-\boldsymbol{Y}(x_k). \tag{2.25}$$

The above equation implies that $\widetilde{\boldsymbol{Y}}(x_k) = \boldsymbol{Y}(x_k)$ and $\left[\widetilde{\boldsymbol{Y}}(x)\right]' = D^-\boldsymbol{Y}(x_k)$.

**Theorem 2.2.** *Let $\boldsymbol{y}$ be the continuous solution of (2.1a)–(2.1b), $\boldsymbol{Y}$ be the discrete solution of (2.9a)–(2.9b). Assuming $\widetilde{\boldsymbol{Y}}(x)$ as the piecewise linear interpolation of $\boldsymbol{Y}(x_k)$, the following inequality holds*

$$\|\widetilde{\boldsymbol{Y}} - \boldsymbol{y}\|_\infty \leq C_1(\lambda_1 + \lambda_2 + \lambda_3 + \lambda_4 + \lambda_5), \tag{2.26}$$

*where* $\lambda_j := \max\limits_{1\leq k\leq N} \lambda_{j,k}, j = 1, \ldots, 5,$

$$\lambda_{1,k} := h_k \max_{1\leq i\leq \ell}\left(\sum_{j=1}^{\ell} |q_{ij}(x_k)||D^-Y_j(x_k)|\right), \qquad \lambda_{2,k} := h_k \max_{1\leq i\leq \ell}\left(\sum_{j=1}^{\ell} |a_{ij}(x_k)||D^-Y_j(x_k)|\right),$$

$$\lambda_{3,k} := h_k \max_{1\leq i\leq \ell}\left(\sum_{j=1}^{\ell} \|a'_{ij}\|_\infty |Y_j(x_k)|\right), \qquad \lambda_{4,k} := h_k^2 \max_{1\leq i\leq \ell}\left(\sum_{j=1}^{\ell} \|a'_{ij}\|_\infty |D^-Y_j(x_k)|\right),$$

$$\lambda_{5,k} := h_k \|\boldsymbol{g}'\|_\infty,$$

*with $q_{ij}$ $(1 \leq i, j \leq \ell)$ the entries of the matrix $Q$.*

**Proof.** For any $x \in (x_{k-1}, x_k)$, $k = 1, 2, \ldots, N$, we have

$$\begin{aligned}
&\mathcal{L}\widetilde{\boldsymbol{Y}}(x) - \mathcal{L}\boldsymbol{y}(x) = \mathcal{E}\left[\widetilde{\boldsymbol{Y}}(x)\right]' + \mathcal{A}(x)\widetilde{\boldsymbol{Y}}(x) - \boldsymbol{g}(x)\\
&= \mathcal{E}D^-\boldsymbol{Y}(x_k) + \left(\mathcal{A}(x_k) + \int_{x_k}^{x} \mathcal{A}'(s)\,ds\right)\left(\boldsymbol{Y}(x_k) + (x-x_k)D^-\boldsymbol{Y}(x_k)\right) - \left(\boldsymbol{g}(x_k) + \int_{x_k}^{x} \boldsymbol{g}'(s)\,ds\right)\\
&= \left\{\mathcal{E}D^-\boldsymbol{Y}(x_k) + \mathcal{A}(x_k)\boldsymbol{Y}(x_k) - \boldsymbol{g}(x_k)\right\} + \mathcal{A}(x_k)(x-x_k)D^-\boldsymbol{Y}(x_k) + \int_{x_k}^{x} \mathcal{A}'(s)\,ds \times \boldsymbol{Y}(x_k)\\
&\quad + (x-x_k)\int_{x_k}^{x} \mathcal{A}'(s)\,ds\, D^-\boldsymbol{Y}(x_k) - \int_{x_k}^{x} \boldsymbol{g}'(s)\,ds\\
&= \left\{\mathcal{E}D^-\boldsymbol{Y}(x_k) + \mathcal{P}(x_k)\boldsymbol{Y}(x_k) - \mathcal{Q}(x_k)\boldsymbol{Y}(x_{k-1}) - \boldsymbol{g}(x_k)\right\} - \mathcal{Q}(x_k)\left\{\boldsymbol{Y}(x_k) - \boldsymbol{Y}(x_{k-1})\right\}\\
&\quad + \mathcal{A}(x_k)(x-x_k)D^-\boldsymbol{Y}(x_k) + \int_{x_k}^{x} \mathcal{A}'(s)\,ds\,\boldsymbol{Y}(x_k) + (x-x_k)\int_{x_k}^{x} \mathcal{A}'(s)\,ds\, D^-\boldsymbol{Y}(x_k) - \int_{x_k}^{x} \boldsymbol{g}'(s)\,ds\\
&= -h_k\mathcal{Q}(x_k)D^-\boldsymbol{Y}(x_k) + \mathcal{A}(x_k)(x-x_k)D^-\boldsymbol{Y}(x_k) + \int_{x_k}^{x} \mathcal{A}'(s)\,ds\,\boldsymbol{Y}(x_k) + (x-x_k)\int_{x_k}^{x} \mathcal{A}'(s)\,ds\\
&\quad \times D^-\boldsymbol{Y}(x_k) - \int_{x_k}^{x} \boldsymbol{g}'(s)\,ds,
\end{aligned} \tag{2.27}$$

where we have used (2.9a) and (2.25) in the above calculations.

Now, we proceed as follows to evaluate each term of (2.27) one by one. First, we have

$$|h_k\mathcal{Q}(x_k)D^-\boldsymbol{Y}(x_k)| \le h_k \max_{1\le i\le \ell}\left(\sum_{j=1}^{\ell} |q_{ij}(x_k)||D^-Y_j(x_k)|\right), \tag{2.28}$$

where $q_{ij}$ $(1 \le i, j \le \ell)$ are the entries of $\mathcal{Q}$. Similarly, it follows that

$$|\mathcal{A}(x_k)(x-x_k)D^-\boldsymbol{Y}(x_k)| \le h_k \max_{1\le i\le \ell}\left(\sum_{j=1}^{\ell} |a_{ij}(x_k)||D^-Y_j(x_k)|\right), \tag{2.29}$$

and

$$\begin{aligned}
\left|\int_{x_k}^{x} \mathcal{A}'(s)\,ds\,\boldsymbol{Y}(x_k)\right| &\le \max_{1\le i\le \ell}\left(\sum_{j=1}^{\ell} \left|\int_{x_k}^{x} a'_{ij}(s)\,ds\, Y_j(x_k)\right|\right)\\
&\le \max_{1\le i\le \ell}\left(\sum_{j=1}^{\ell} \|a'_{ij}\|_\infty \int_{x_k}^{x} ds\,|Y_j(x_k)|\right)\\
&\le h_k \max_{1\le i\le \ell}\left(\sum_{j=1}^{\ell} \|a'_{ij}\|_\infty |Y_j(x_k)|\right).
\end{aligned} \tag{2.30}$$

Following the above arguments, we have the following bound for the next term

$$\begin{aligned}
|(x-x_k)\int_{x_k}^{x} \mathcal{A}'(s)\,ds\, D^-\boldsymbol{Y}(x_k)| &\le h_k \left|\int_{x_k}^{x} \mathcal{A}'(s)\,ds\, D^-\boldsymbol{Y}(x_k)\right|\\
&\le h_k^2 \max_{1\le i\le \ell}\left(\sum_{j=1}^{\ell} \|a'_{ij}\|_\infty |D^-Y_j(x_k)|\right).
\end{aligned} \tag{2.31}$$

Lastly, we have

$$\Big|\int_{x_k}^{x} \boldsymbol{g}'(s)\,ds\Big| \le h_k\|\boldsymbol{g}'\|_\infty. \tag{2.32}$$

Consequently, the required estimate (2.26) can be obtained by combining all these findings from (2.27)–(2.32) in (2.27), and using (2.5). □

## 3. A nonlinear coupled system

### 3.1. The continuous problem and its stability

We consider the following class of SPDEs, which consists of a system of $\ell$ first-order nonlinear differential equations of the form

$$\begin{cases} \boldsymbol{\mathcal{T}}\boldsymbol{y} := \mathcal{E}\boldsymbol{y}'(x) + \boldsymbol{b}(x,\boldsymbol{y}(x)) = \boldsymbol{0}, & x\in\Omega=(0,1], \quad \text{(a)}\\ \boldsymbol{y}(0) = \boldsymbol{\gamma}^\star, & \text{(b)} \end{cases} \tag{3.1}$$

where the solution vector is $\boldsymbol{y}(x) = \big(y_1,\dots,y_\ell\big)^T$, $\boldsymbol{b}(x,\boldsymbol{y}(x)) = \big(b_1(x,\boldsymbol{y}(x)),\dots,b_\ell(x,\boldsymbol{y}(x))\big)^T \in (C^2(\overline{\Omega}\times\mathbb{R}^\ell))^\ell$ and $\boldsymbol{\gamma}^\star$ is a given $\ell$-column constant vector. Furthermore, $\boldsymbol{\mathcal{T}} = (\mathcal{T}_1,\dots,\mathcal{T}_\ell)^T$ with $\mathcal{T}_i\boldsymbol{y} := \epsilon_i y_i'(x) + b_i(x,\boldsymbol{y}(x)) = 0,\ i=1,\dots,\ell$, and for all $(x,\boldsymbol{y})\in\overline{\Omega}\times\mathbb{R}^\ell$, we assume that

$$\begin{cases} \frac{\partial b_m}{\partial y_i} \le 0,\ m\ne i; \quad \frac{\partial b_m}{\partial y_i} > 0,\ m=i; \quad m,i\in\{1,\dots,\ell\}, & \text{(a)}\\ \sum_{i=1}^{\ell} \frac{\partial b_m}{\partial y_i} > \beta > 0, \quad m=1,\dots,\ell. & \text{(b)} \end{cases} \tag{3.2}$$

The implicit function theorem and assumptions (3.2a)–(3.2b) guarantee that there is a unique solution $\boldsymbol{y}$ to the nonlinear problem (3.1a)–(3.1b) and also that the reduced problem is given by $\boldsymbol{b}(x,\boldsymbol{y}_0)=\boldsymbol{0}$, $x\in\Omega$.

Let us define the Jacobian matrix $\boldsymbol{J}(x,\boldsymbol{y}) := \left(\frac{\partial b_m}{\partial y_i}(x,\boldsymbol{y})\right)\ \forall\ 1\le i,m\le\ell$. It is clear from the conditions (3.2a)–(3.2b) that $\boldsymbol{J}$ is an M-matrix for all $(x,\boldsymbol{y})\in\overline{\Omega}\times\mathbb{R}^\ell$. For any vector valued functions $\boldsymbol{u}$ and $\boldsymbol{v}$, we define

$$\boldsymbol{\mathcal{J}}_{[\boldsymbol{u};\boldsymbol{v}]}(x) := \int_{s=0}^{1} \boldsymbol{J}\big(x,\boldsymbol{v}(x)+s(\boldsymbol{u}(x)-\boldsymbol{v}(x)\big)\,ds.$$

An application of the mean value theorem gives

$$\boldsymbol{b}(x,\boldsymbol{u}(x)) - \boldsymbol{b}(x,\boldsymbol{v}(x)) = \int_{s=0}^{1} \frac{d}{ds}\Big(\boldsymbol{b}(x,\boldsymbol{v}(x)+s(\boldsymbol{u}(x)-\boldsymbol{v}(x))\Big)\,ds = \boldsymbol{\mathcal{J}}_{[\boldsymbol{u};\boldsymbol{v}]}(x)(\boldsymbol{u}-\boldsymbol{v}).$$

Now, we define the following linear operator

$$\widetilde{\boldsymbol{\mathcal{T}}}_{[\boldsymbol{u};\boldsymbol{v}]}\boldsymbol{y} := \mathcal{E}\boldsymbol{y}'(x) + \boldsymbol{\mathcal{J}}_{[\boldsymbol{u};\boldsymbol{v}]}(x)\boldsymbol{y}(x), \quad x\in\Omega. \tag{3.3}$$

The operator $\widetilde{\boldsymbol{\mathcal{T}}}_{[\boldsymbol{u};\boldsymbol{v}]}$ satisfies the following continuous maximum principle.

**Lemma 3.1** *(Continuous maximum principle). Suppose that* $\boldsymbol{y} = \big(y_1,\dots,y_\ell\big)^T$ *satisfies* $\boldsymbol{y}(0)\ge\boldsymbol{0}$ *and* $\widetilde{\boldsymbol{\mathcal{T}}}_{[\boldsymbol{u};\boldsymbol{v}]}\boldsymbol{y}(x)\ge\boldsymbol{0}\ \forall\ x\in\Omega$. *Then* $\boldsymbol{y}(x)\ge\boldsymbol{0}\ \forall\ x\in\overline{\Omega}$.

**Proof.** Let $y_i(r_i) = \min\limits_{x\in\overline{\Omega}}\{y_i(x)\}$, for $1\le i\le\ell$. Without any loss of generality, we can consider that $y_1(r_1)\le y_i(r_i)$, for $2\le i\le\ell$. If $y_1(r_1)\ge 0$, then nothing needs to be proved. On the contrary, we assume that $y_1(r_1)<0$. Clearly it implies that $r_1\ne 0$ and $y_1'(r_1)=0$. Under the problem assumptions (3.2a)–(3.2b), for $m=1$, we observe that

$$\frac{\partial b_1}{\partial y_1} + \frac{\partial b_1}{\partial y_2} + \cdots + \frac{\partial b_1}{\partial y_\ell} > 0.$$

Hence, we have

$$\begin{aligned} \frac{\partial b_1}{\partial y_1}\cdot y_1(r_1) &< -\frac{\partial b_1}{\partial y_2}\cdot y_1(r_1) - \cdots - \frac{\partial b_1}{\partial y_\ell}\cdot y_1(r_1) \qquad (\because y_1(r_1)<0)\\ &\le -\frac{\partial b_1}{\partial y_2}\cdot y_2(r_2) - \cdots - \frac{\partial b_1}{\partial y_\ell}\cdot y_\ell(r_\ell) \qquad (\because y_1(r_1)\le y_i(r_i),\ \forall\ 2\le i\le\ell). \end{aligned}$$

Thus, it holds

$$\frac{\partial b_1}{\partial y_1}\cdot y_1(r_1)+\frac{\partial b_1}{\partial y_2}\cdot y_2(r_1)+\cdots+\frac{\partial b_1}{\partial y_\ell}\cdot y_\ell(r_1)\le 0, \tag{3.4}$$

where we have used the fact that $y_i(r_i)\le y_i(r_1)$. Thus, it follows from (3.3) and (3.4) that $\left(\widetilde{\boldsymbol{\mathcal{T}}}_{[\boldsymbol{u};\boldsymbol{v}]}\boldsymbol{y}_1(r_1)\right)<0$, which leads to a contradiction and thereby yields the required result. □

After subtracting $\boldsymbol{b}(x,\boldsymbol{0})$ from both sides of (3.1a) and using (3.3) with $\boldsymbol{u}\equiv\boldsymbol{y},\boldsymbol{v}\equiv\boldsymbol{0}$, we get the linearized form of (3.1a) as follows

$$\widetilde{\boldsymbol{\mathcal{T}}}\boldsymbol{y}:=\widetilde{\boldsymbol{\mathcal{T}}}_{[\boldsymbol{y};\boldsymbol{0}]}\boldsymbol{y}=\mathcal{E}\boldsymbol{y}'(x)+\boldsymbol{\mathcal{J}}_{[\boldsymbol{y};\boldsymbol{0}]}(x)\boldsymbol{y}(x)=-\boldsymbol{b}(x,\boldsymbol{0}),\quad x\in\Omega. \tag{3.5}$$

Clearly, the operator $\widetilde{\boldsymbol{\mathcal{T}}}$ also satisfies the maximum principle (Lemma 3.1). Next, we prove the following result, which will be used in a later subsection for the a posteriori error analysis of the considered nonlinear problem.

**Corollary 3.1.** *Consider a bounded piecewise vector function* $\boldsymbol{\aleph}$ *such that* $\boldsymbol{\mathcal{T}}\widehat{\boldsymbol{y}}-\boldsymbol{\mathcal{T}}\widetilde{\boldsymbol{y}}=\boldsymbol{\aleph}$ *where* $\widehat{\boldsymbol{y}}=\left(\widehat{y}_1,\ldots,\widehat{y}_\ell\right)^T$ *and* $\widetilde{\boldsymbol{y}}=\left(\widetilde{y}_1,\ldots,\widetilde{y}_\ell\right)^T$ *are any two functions satisfying the initial condition* $\widehat{\boldsymbol{y}}(0)=\widetilde{\boldsymbol{y}}(0)$. *Then, we have*

$$\|\widehat{\boldsymbol{y}}-\widetilde{\boldsymbol{y}}\|_\infty\le C_2\|\boldsymbol{\mathcal{T}}\widehat{\boldsymbol{y}}-\boldsymbol{\mathcal{T}}\widetilde{\boldsymbol{y}}\|_\infty. \tag{3.6}$$

**Proof.** Note that $(\widehat{\boldsymbol{y}}-\widetilde{\boldsymbol{y}})(0)=\boldsymbol{0}$. Using the standard linearization technique, it is not hard to see that $\boldsymbol{\aleph}=\boldsymbol{\mathcal{T}}\widehat{\boldsymbol{y}}-\boldsymbol{\mathcal{T}}\widetilde{\boldsymbol{y}}=\widetilde{\boldsymbol{\mathcal{T}}}_{[\widehat{\boldsymbol{y}};\widetilde{\boldsymbol{y}}]}\left(\widehat{\boldsymbol{y}}-\widetilde{\boldsymbol{y}}\right)$, where the operator $\widetilde{\boldsymbol{\mathcal{T}}}$ is defined in (3.3). Now, we assume the following vector barrier function

$$\boldsymbol{\Theta}^{\pm}(x)=\frac{1}{\beta}\|\widetilde{\boldsymbol{\mathcal{T}}}_{[\widehat{\boldsymbol{y}};\widetilde{\boldsymbol{y}}]}\left(\widehat{\boldsymbol{y}}-\widetilde{\boldsymbol{y}}\right)\|_\infty\pm\left(\widehat{\boldsymbol{y}}-\widetilde{\boldsymbol{y}}\right)(x),\quad x\in\overline{\Omega}.$$

Clearly, $\boldsymbol{\Theta}^{\pm}(0)\ge\boldsymbol{0}$ and $\widetilde{\boldsymbol{\mathcal{T}}}_{[\widehat{\boldsymbol{y}};\widetilde{\boldsymbol{y}}]}\boldsymbol{\Theta}^{\pm}(x)\ge\boldsymbol{0}$ for $x\in\Omega$. Then, Lemma 3.1 yields $\boldsymbol{\Theta}^{\pm}(x)\ge\boldsymbol{0}$ for $x\in\overline{\Omega}$. Thus,

$$\|\widehat{\boldsymbol{y}}-\widetilde{\boldsymbol{y}}\|_\infty\le\frac{1}{\beta}\|\widetilde{\boldsymbol{\mathcal{T}}}_{[\widehat{\boldsymbol{y}};\widetilde{\boldsymbol{y}}]}\left(\widehat{\boldsymbol{y}}-\widetilde{\boldsymbol{y}}\right)\|_\infty=C_2\|\boldsymbol{\mathcal{T}}\widehat{\boldsymbol{y}}-\boldsymbol{\mathcal{T}}\widetilde{\boldsymbol{y}}\|_\infty.\quad\square$$

In order to deduce the a priori error estimate of the nonlinear continuous problem (3.1a)–(3.1b), we require the derivative bounds of $\boldsymbol{y}$. For this purpose, we decompose the continuous solution $\boldsymbol{y}$ as $\boldsymbol{y}=\boldsymbol{v}+\boldsymbol{w}$, where $\boldsymbol{v}$ and $\boldsymbol{w}$ are the regular and the singular parts, respectively. Further, the regular part $\boldsymbol{v}$ satisfies

$$\mathcal{E}\boldsymbol{v}'+\boldsymbol{b}(x,\boldsymbol{v})=\boldsymbol{0}\ \text{ in }\Omega,\quad \boldsymbol{v}(0)=\boldsymbol{y}_0(0), \tag{3.7}$$

while the singular part $\boldsymbol{w}$ is the solution of

$$\mathcal{E}\boldsymbol{w}'+\boldsymbol{b}(x,\boldsymbol{v}+\boldsymbol{w})-\boldsymbol{b}(x,\boldsymbol{v})=\boldsymbol{0}\ \text{ in }\Omega,\quad \boldsymbol{w}(0)=\boldsymbol{y}(0)-\boldsymbol{v}(0). \tag{3.8}$$

Let the matrix $\mathcal{E}_k$ be the zero matrix except that on the main diagonal $(\mathcal{E}_k)_{ii}=\epsilon_i, i\ge k$. With this notation, note that $\mathcal{E}_1=\mathcal{E}$. Let $\boldsymbol{e}_k$ be the $k^{\text{th}}$ vector of the canonical basis.

To obtain appropriate bounds on the regular component $\boldsymbol{v}$, we follow the ideas given in [29,30]. Now, we assume the further decomposition of $\boldsymbol{v}$ as $\boldsymbol{v}=\sum_{k=1}^{\ell}\boldsymbol{\eta}^{[k]}$, where $\boldsymbol{\eta}^{[k]}$ are the solutions of the problems

$$\mathcal{E}_\ell\frac{d\boldsymbol{\eta}^{[\ell]}}{dx}+\boldsymbol{b}(x,\boldsymbol{\eta}^{[\ell]})=\boldsymbol{0}\ \text{ in }\Omega,\quad \eta_\ell^{[\ell]}(0)=v_\ell(0), \tag{3.9}$$

$$\mathcal{E}_i\frac{d\boldsymbol{\eta}^{[i]}}{dx}+\boldsymbol{b}\left(x,\sum_{k=i}^{\ell}\boldsymbol{\eta}^{[k]}\right)-\boldsymbol{b}\left(x,\sum_{k=i+1}^{\ell}\boldsymbol{\eta}^{[k]}\right)=-\epsilon_i\sum_{k=i+1}^{\ell}\frac{d\eta_i^{[k]}}{dx}\boldsymbol{e}_i\ \text{ in }\Omega, \tag{3.10}$$

$$\eta_k^{[i]}(0)=0,\quad i\le k\le\ell,\ 1\le i<\ell. \tag{3.11}$$

**Lemma 3.2.** *The regular part* $\boldsymbol{v}$ *satisfies*

$$\|\boldsymbol{v}^{(m)}\|_\infty\le C,\ \text{ for } m=0,1,\quad \|v_k^{(2)}\|_\infty\le C\epsilon_k^{-1},\ \text{ for } k=1,\ldots,\ell.$$

**Proof.** Assumptions (3.2a)–(3.2b) imply that $\boldsymbol{\eta}^{[\ell]}(0)=\boldsymbol{v}(0)$, and $\boldsymbol{\eta}^{[i]}(0)=\boldsymbol{0}$, $1\le i<\ell$. Letting $\boldsymbol{\phi}=\boldsymbol{\eta}^{[\ell]}-\boldsymbol{y}_0$, we see that $\boldsymbol{\phi}$ is the solution of

$$\mathcal{E}_\ell\boldsymbol{\phi}'+\boldsymbol{\mathcal{J}}_{[\boldsymbol{\eta}^{[\ell]};\boldsymbol{y}_0]}(x)\,\boldsymbol{\phi}=-\mathcal{E}_\ell\boldsymbol{y}_0'\ \text{ in }\Omega,\quad \boldsymbol{\phi}(0)=0.$$

Assumptions (3.2a)–(3.2b) ensure that the above system satisfies the maximum principle. Consequently $\|\boldsymbol{\phi}\|_\infty\le C\epsilon_\ell$ and hence $\|\phi_\ell'\|_\infty\le C$. Using $\boldsymbol{\eta}^{[\ell]}=\boldsymbol{\phi}+\boldsymbol{y}_0$, we get

$$\|\boldsymbol{\eta}^{[\ell]}\|_\infty \le C \ \text{ and } \ \left\| \frac{d\boldsymbol{\eta}_\ell^{[\ell]}}{dx} \right\|_\infty \le C.$$

Now we use that $b_1(x,\boldsymbol{\eta}^{[\ell]}) = \cdots = b_{\ell-1}(x,\boldsymbol{\eta}^{[\ell]}) = 0$, to get $\|\frac{d\eta_k^{[\ell]}}{dx}\|_\infty \le C$, $1 \le k < \ell$. Differentiating the $\ell^{th}$ equation of (3.9) and using the bounds for lower-order derivatives of $\boldsymbol{\eta}^{[\ell]}$, we get $\|\frac{d^2\eta_\ell^{[\ell]}}{dx^2}\|_\infty \le C\epsilon_\ell^{-1}$. Now we use the first $\ell-1$ equations of (3.9) to get $\|\frac{d^2\eta_k^{[\ell]}}{dx^2}\|_\infty \le C\epsilon_\ell^{-1}$, $1 \le k < \ell$. Next, we estimate $\boldsymbol{\eta}^{[i]}$, $1 \le i < \ell$, which is the solution of the problem

$$\mathcal{E}_i \frac{d\boldsymbol{\eta}^{[i]}}{dx} + \boldsymbol{\mathcal{J}}_{[\sum_{k=i}^{\ell}\boldsymbol{\eta}^{[k]};\sum_{k=i+1}^{\ell}\boldsymbol{\eta}^{[k]}(x)]}\boldsymbol{\eta}^{[i]} = -\epsilon_i \sum_{k=i+1}^{\ell} \frac{d\eta_i^{[k]}}{dx}\boldsymbol{e}_i \ \text{ in } \Omega,$$

$$\eta_k^{[i]}(0) = 0, \ \ i \le k \le \ell.$$

On applying the maximum principle, we get $\|\boldsymbol{\eta}^{[i]}\|_\infty \le C\epsilon_i$.

Hence, it holds $\|\frac{d\eta_k^{[i]}}{dx}\|_\infty \le C(\epsilon_i\epsilon_k^{-1})$, $i \le k \le \ell$. Consequently $\|\frac{d\eta_k^{[i]}}{dx}\|_\infty \le C$, $1 \le k \le i-1$ (if $i > 1$). Differentiating (3.10) and using the previous estimates, we get $\|\frac{d^2\eta_k^{[i]}}{dx^2}\|_\infty \le C\epsilon_k^{-1}$, $k = 1,\ldots,\ell$. On combining the bounds of $\boldsymbol{\eta}^{[i]}, i = 1,\ldots,\ell$, we get the required estimate for $\boldsymbol{v}$. □

**Lemma 3.3.** *The singular part $\boldsymbol{w}$ satisfies*

$$|w_i(x)| \le C\exp\left(-\frac{\beta x}{\epsilon_\ell}\right), \quad |w_i'(x)| \le C\sum_{k=i}^{\ell}\epsilon_k^{-1}\exp\left(-\frac{\beta x}{\epsilon_k}\right), \quad \epsilon_i|w_i''(x)| \le C\sum_{k=1}^{\ell}\epsilon_k^{-1}\exp\left(-\frac{\beta x}{\epsilon_k}\right),$$

*for $i = 1,\ldots,\ell$.*

**Proof.** Using the mean-value theorem in (3.8), we can get

$$\widetilde{\boldsymbol{\mathcal{T}}}_{[\boldsymbol{v}+\boldsymbol{w};\boldsymbol{v}]}\boldsymbol{w} := \boldsymbol{\mathcal{E}}\boldsymbol{w}' + \boldsymbol{\mathcal{J}}_{[\boldsymbol{v}+\boldsymbol{w};\boldsymbol{v}]}\boldsymbol{w} = \boldsymbol{0} \ \text{ in } \Omega, \ \ \boldsymbol{w}(0) = \boldsymbol{y}(0) - \boldsymbol{v}(0). \tag{3.12}$$

We consider the barrier function $\boldsymbol{\Psi}^{\pm}(x) = \boldsymbol{C}\exp\left(-\frac{\beta x}{\epsilon_\ell}\right) \pm \boldsymbol{w}(x)$, where the constant vector $\boldsymbol{C}$ is chosen sufficiently large such that $\boldsymbol{\Psi}^{\pm}(0) \ge |\boldsymbol{w}(0)|$. Clearly, $\boldsymbol{\Psi}^{\pm}(0) \ge \boldsymbol{0}$, and we have

$$\widetilde{\boldsymbol{\mathcal{T}}}_{[\boldsymbol{v}+\boldsymbol{w};\boldsymbol{v}]}\boldsymbol{\Psi}^{\pm}(x) = \left(-\frac{\beta}{\epsilon_\ell}\boldsymbol{\mathcal{E}} + \boldsymbol{\mathcal{J}}_{[\boldsymbol{v}+\boldsymbol{w};\boldsymbol{v}]}\right)\boldsymbol{C}\exp\left(-\frac{\beta x}{\epsilon_\ell}\right).$$

Thus, for the $i^{th}$ component, it holds

$$\left(\widetilde{\boldsymbol{\mathcal{T}}}_{[\boldsymbol{v}+\boldsymbol{w};\boldsymbol{v}]}\boldsymbol{\Psi}^{\pm}\right)_i = C\left(\sum_{k=1}^{\ell}\frac{\partial b_i}{\partial y_k} - \beta\frac{\epsilon_i}{\epsilon_\ell}\right)\exp\left(-\frac{\beta x}{\epsilon_\ell}\right) \ge 0, \qquad \text{(from (3.2b))}.$$

Therefore, from Lemma 3.1, it follows that $\boldsymbol{\Psi}^{\pm}(x) \ge 0$. Consequently, we obtain the following bound on the components $w_i(x)$, $i = 1,\ldots,\ell$

$$|w_i(x)| \le C\exp\left(-\frac{\beta x}{\epsilon_\ell}\right), \quad i = 1,\ldots,\ell. \tag{3.13}$$

Next, we derive the first-derivative bound of $\boldsymbol{w}$. For this, we consider the last equation of (3.12), i.e.

$$\epsilon_\ell w_\ell'(x) + \sum_{k=1}^{\ell}\left(\int_0^1 \frac{\partial b_\ell}{\partial y_k}(x, \boldsymbol{v} + s\boldsymbol{w})\,ds \cdot w_k\right) = 0.$$

After using (3.13) in the above equation, we get the following first-derivative bound of the $\ell^{th}$ component of $\boldsymbol{w}$

$$|w_\ell'(x)| \le C\epsilon_\ell^{-1}\exp\left(-\frac{\beta x}{\epsilon_\ell}\right). \tag{3.14}$$

Now, we establish the bound of $w_i'$ for $1 \le i \le \ell-1$. For this, we consider the following system of equations in matrix form

$$\widetilde{\boldsymbol{\mathcal{T}}}_{[\boldsymbol{v}+\boldsymbol{w};\boldsymbol{v}]}\widehat{\boldsymbol{w}} := \widehat{\boldsymbol{\mathcal{E}}}\widehat{\boldsymbol{w}}' + \widehat{\boldsymbol{\mathcal{J}}}_{[\boldsymbol{v}+\boldsymbol{w};\boldsymbol{v}]}\widehat{\boldsymbol{w}} = \widehat{\boldsymbol{f}}, \quad \widehat{\boldsymbol{w}}(0) = \boldsymbol{y}(0) - \boldsymbol{v}(0), \tag{3.15}$$

where the matrices $\widehat{\mathcal{E}}$ and $\widehat{\boldsymbol{\mathcal{J}}}_{[\boldsymbol{v}+\boldsymbol{w};\boldsymbol{v}]}$ are obtained by removing the last row and column of $\mathcal{E}$ and $\boldsymbol{\mathcal{J}}_{[\boldsymbol{v}+\boldsymbol{w};\boldsymbol{v}]}$, respectively. Further, $\widehat{\boldsymbol{w}} = \left(w_1, \ldots, w_{\ell-1}\right)$ and the entries of $\widehat{\boldsymbol{f}}$ are given by $\widehat{f}_i = -\int_0^1 \frac{\partial b_i}{\partial y_\ell}(x, \boldsymbol{v} + s\boldsymbol{w})\, ds \cdot w_\ell$ for $1 \le i \le \ell - 1$. Using the bounds (3.13) and (3.14), we get

$$|\widehat{f}_i(x)| \le C|w_\ell(x)| \le C \exp\left(-\frac{\beta x}{\epsilon_\ell}\right),$$
$$|\widehat{f}_i'(x)| \le C|w_\ell'(x)| \le C\epsilon_\ell^{-1} \exp\left(-\frac{\beta x}{\epsilon_\ell}\right),$$

for $i = 1, \ldots, \ell$. Now, we consider the decomposition of $\widehat{\boldsymbol{w}} = \widehat{\boldsymbol{w}}_r + \widehat{\boldsymbol{w}}_s$, into regular and singular components, where

$$\begin{cases} \widetilde{\boldsymbol{\mathcal{T}}}_{[\boldsymbol{v}+\boldsymbol{w};\boldsymbol{v}]}\widehat{\boldsymbol{w}}_r = \widehat{\boldsymbol{f}}, \quad \widehat{\boldsymbol{w}}_r(0) = \left(\widehat{\boldsymbol{\mathcal{J}}}_{[\boldsymbol{v}+\boldsymbol{w};\boldsymbol{v}]}\right)^{-1}\widehat{\boldsymbol{f}}, \\ \widetilde{\boldsymbol{\mathcal{T}}}_{[\boldsymbol{v}+\boldsymbol{w};\boldsymbol{v}]}\widehat{\boldsymbol{w}}_s = \boldsymbol{0}, \quad \widehat{\boldsymbol{w}}_s(0) = \widehat{\boldsymbol{w}}(0) - \widehat{\boldsymbol{w}}_r(0). \end{cases}$$

We take another barrier function defined by $\boldsymbol{\Psi}^{\pm}(x) = \boldsymbol{C}\exp\left(-\frac{\beta x}{\epsilon_\ell}\right) \pm \widehat{\boldsymbol{w}}_r(x)$. Clearly, $\boldsymbol{\Psi}^{\pm}(0) \ge \boldsymbol{0}$ and $\widetilde{\boldsymbol{\mathcal{T}}}_{[\boldsymbol{v}+\boldsymbol{w};\boldsymbol{v}]}\boldsymbol{\Psi}^{\pm}(x) > \boldsymbol{0}$. Thus, from Lemma 3.1 and using the bound on $\widehat{f}_i$ we obtain $\boldsymbol{\Psi}^{\pm}(x) \ge \boldsymbol{0}$, and therefore, it holds

$$|\widehat{w}_{r,i}(x)| \le C\exp\left(-\frac{\beta x}{\epsilon_\ell}\right), \quad i = 1, \ldots, \ell. \tag{3.16}$$

By following a similar argument for the barrier function $\boldsymbol{\theta}^{\pm}(x) = \boldsymbol{C}\epsilon_\ell^{-1}\exp\left(-\frac{\beta x}{\epsilon_\ell}\right) \pm \widehat{\boldsymbol{w}}_r'$ and using the bound on $\widehat{f}'$, we get

$$|\widehat{w}_{r,i}'(x)| \le C\epsilon_\ell^{-1}\exp\left(-\frac{\beta x}{\epsilon_\ell}\right), \quad i = 1, \ldots, \ell. \tag{3.17}$$

Now we use the mathematical induction. We suppose that the first-derivative bounds hold for all systems with $\ell - 1$ equations. Consequently, we can have the following result for $\widehat{\boldsymbol{w}}_s$

$$|\widehat{w}_{s,i}'(x)| \le C\sum_{k=i}^{\ell-1}\epsilon_k^{-1}\exp\left(-\frac{\beta x}{\epsilon_k}\right), \quad i = 1, \ldots, \ell - 1. \tag{3.18}$$

Combining the bounds (3.17) and (3.18) we get

$$|\widehat{w}_i'(x)| \le C\sum_{k=i}^{\ell}\epsilon_k^{-1}\exp\left(-\frac{\beta x}{\epsilon_k}\right),$$

and recalling the definition of $\widehat{\boldsymbol{w}}$ we have

$$|w_i'(x)| \le C\sum_{k=i}^{\ell}\epsilon_k^{-1}\exp\left(-\frac{\beta x}{\epsilon_k}\right). \tag{3.19}$$

We have thus proved that the first derivative bound is true for the system with $\ell$ equations. Therefore, we can conclude by the mathematical induction that the first derivative bound is true for any system with $\ell > 1$ equations. At last, the second derivative bound is proved by differentiating (3.12) and using the previous bounds obtained for $\boldsymbol{w}$ and $\boldsymbol{w}'$. □

### 3.2. The discrete problem

We propose two splitting difference schemes for the nonlinear system (3.1a)–(3.1b) on an arbitrary grid $\overline{\Omega}^N$ as follows

$$\begin{cases} \left[\boldsymbol{\mathcal{T}}^N\boldsymbol{Y}\right]_k := \left(\left[\mathcal{T}_1^N\boldsymbol{Y}\right]_k, \left[\mathcal{T}_2^N\boldsymbol{Y}\right]_k, \ldots, \left[\mathcal{T}_N^N\boldsymbol{Y}\right]_k\right)^T = \boldsymbol{0}, & \text{(a)} \\ \boldsymbol{Y}_0 = \boldsymbol{\gamma}^\star, & \text{(b)} \end{cases} \tag{3.20}$$

where the operator $D^-$ is given in (2.10), and for $1 \le i \le \ell$, the operators $\mathcal{T}_i^N$ are defined by

**Scheme I** :

$$\left[\mathcal{T}_i^N\boldsymbol{Y}\right]_k := \epsilon_i D^- Y_i(x_k) + b_i(x_k, Y_1(x_{k-1}), \ldots, Y_{i-1}(x_{k-1}), Y_i(x_k), Y_{i+1}(x_{k-1}), \ldots, Y_\ell(x_{k-1})). \tag{3.21}$$

**Scheme II** :

$$\left[\mathcal{T}_i^N\boldsymbol{Y}\right]_k := \epsilon_i D^- Y_i(x_k) + b_i(x_k, Y_1(x_k), \ldots, Y_{i-1}(x_k), Y_i(x_k), Y_{i+1}(x_{k-1}), \ldots, Y_\ell(x_{k-1})). \tag{3.22}$$

To ease the analysis in subsequent subsections, we provide the following general form of the proposed schemes

$$\left[\mathcal{T}_i^N \boldsymbol{Y}\right]_k := \epsilon_i D^- Y_i(x_k) + b_i(x_k, Y_1(x_{k-\varrho}), \dots, Y_{i-1}(x_{k-\varrho}), Y_i(x_k), Y_{i+1}(x_{k-1}), \dots, Y_\ell(x_{k-1})), \tag{3.23}$$

where $\varrho$ can be 0 or 1. Thus, when $\varrho = 1$, the above equation corresponds to Scheme I and for $\varrho = 0$, it corresponds to Scheme II.

### 3.3. A priori error analysis

We now prove the a priori error estimate of the nonlinear discrete scheme defined by (3.23). For this purpose, let $\boldsymbol{Z} = \boldsymbol{y} - \boldsymbol{Y}$ be the error vector corresponding to the discrete scheme given by (3.23). Then, the $i^{\text{th}}$-component of the error function $Z_i$ will be the solution of the problem

$$\begin{aligned}\epsilon_i D^- Z_i(x_k) + b_i(x_k, y_1(x_k), \dots, y_\ell(x_k)) - b_i(x_k, Y_1(x_{k-\varrho}), \dots, Y_{i-1}(x_{k-\varrho}), Y_i(x_k), Y_{i+1}(x_{k-1}), \dots, Y_\ell(x_{k-1})) \\ = \epsilon_i \left(D^- y_i(x) - \frac{d}{dx} y_i(x)\right)\Big|_{x=x_k}, \ Z_i(0) = 0, \ 1 \le k \le N,\end{aligned}$$

which can be rewritten as

$$\epsilon_i D^- Z_i(x_k) + \bar{a}_{i,i}(x_k) Z_i(x_k) + \sum_{m=1}^{i-1} \bar{a}_{i,m}(x_k) Z_m(x_{k-\varrho}) + \sum_{m=i+1}^{\ell} \bar{a}_{i,m}(x_k) Z_m(x_{k-1}) = \chi_i(x_k), \ Z_i(0) = 0,$$

where the coefficients are given by

$$\bar{a}_{i,m}(x_k) = \frac{\partial b_i}{\partial u_m}\Big(x_k, v_{1,k}, \dots, v_{i-1,k}, v_{i,k}, v_{i+1,k}, \dots, v_{\ell,k}\Big),$$

and $v_{m,k}$ are the intermediate values. The remainder term is given by

$$\begin{aligned}\chi_i(x_k) = \epsilon_i \left(D^- y_i(x) - \frac{d}{dx} y_i(x)\right)\Big|_{x=x_k} - \sum_{m=1}^{i-1} \tilde{\mathcal{R}}_{i,m}(x_k)(y_m(x_k) - y_m(x_{k-\varrho})) \\ - \sum_{m=i+1}^{\ell} \tilde{\mathcal{R}}_{i,m}(x_k)(y_m(x_k) - y_m(x_{k-1})),\end{aligned} \tag{3.24}$$

where, for Scheme I, $\tilde{\mathcal{R}}_{i,m}(x_k) = \tilde{a}_{i,m}(x_k)$ with

$$\tilde{a}_{i,m}(x_k) = \frac{\partial b_i}{\partial u_m}\Big(x_k, \tilde{v}_{1,k}, \dots, \tilde{v}_{i-1,k}, y_i(x_k), \tilde{v}_{i+1,k}, \dots, \tilde{v}_{\ell,k}\Big),$$

where $\tilde{v}_{m,k}$ are the intermediate values, while for Scheme II, $\tilde{\mathcal{R}}_{i,m}(x_k) = 0, m = 1, \dots, i-1$, and $\tilde{\mathcal{R}}_{i,m}(x_k) = \tilde{a}_{i,m}(x_k), m = i+1, \dots, \ell$, with

$$\tilde{a}_{i,m}(x_k) = \frac{\partial b_i}{\partial u_m}\Big(x_k, y_1(x_k), \dots, y_{i-1}(x_k), y_i(x_k), \tilde{v}_{i+1,k}, \dots, \tilde{v}_{\ell,k}\Big),$$

where $\tilde{v}_{m,k}$ are the intermediate values. Note that for Scheme II the middle term in (3.24) will be absent.

Now, we define a linear discrete operator $[\hat{\mathcal{T}}^N \boldsymbol{\Psi}]_k := ([\hat{\mathcal{T}}_1^N \boldsymbol{\Psi}]_k, \dots, [\hat{\mathcal{T}}_\ell^N \boldsymbol{\Psi}]_k)^T$, where

$$[\hat{\mathcal{T}}_i^N \boldsymbol{\Psi}]_k := \epsilon_i D^- \Psi_i(x_k) + \bar{a}_{i,i}(x_k)\Psi_i(x_k) + \sum_{m=1}^{i-1} \bar{a}_{i,m}(x_k)\Psi_m(x_{k-\varrho}) + \sum_{m=i+1}^{\ell} \bar{a}_{i,m}(x_k)\Psi_m(x_{k-1}), \ 1 \le k \le N.$$

The discrete operator $\hat{\mathcal{T}}^N$ satisfies the following discrete maximum principle.

**Lemma 3.4** *(Discrete Maximum Principle). For any vector mesh function $\boldsymbol{\Psi} = (\Psi_1, \dots, \Psi_\ell)^T$ satisfying $\boldsymbol{\Psi}_0 \ge \boldsymbol{0}$ and $[\hat{\mathcal{T}}^N \boldsymbol{\Psi}]_k \ge \boldsymbol{0}, 1 \le k \le N$, we have $\boldsymbol{\Psi}_k \ge \boldsymbol{0}$ for $k = 0, 1, \dots, N$.*

**Proof.** Let $\mathcal{M}$ be the matrix associated to the discrete operator $\hat{\mathcal{T}}^N$. Then

$$\mathcal{M}\boldsymbol{\Psi} = \left(\Psi_{1,0}, [\hat{\mathcal{T}}_1^N \boldsymbol{\Psi}]_1, \dots, [\hat{\mathcal{T}}_1^N \boldsymbol{\Psi}]_N, \Psi_{2,0}, [\hat{\mathcal{T}}_2^N \boldsymbol{\Psi}]_1, \dots, [\hat{\mathcal{T}}_2^N \boldsymbol{\Psi}]_N, \dots, \Psi_{\ell,0}, [\hat{\mathcal{T}}_\ell^N \boldsymbol{\Psi}]_1, \dots, [\hat{\mathcal{T}}_\ell^N \boldsymbol{\Psi}]_N\right)^T.$$

From the assumption (3.2a), it can be observed that $\bar{a}_{i,i} > 0$ and $\bar{a}_{i,m} \le 0$. Thus, one can easily deduce that the matrix $\mathcal{M}$ is diagonally dominant and has non-positive off-diagonal entries. Consequently, $\mathcal{M}$ is an $M$-matrix and has positive inverse, i.e., $\mathcal{M}^{-1} \ge 0$ ([31]). Using this with $\boldsymbol{\Psi}_0 \ge \boldsymbol{0}$, and $[\hat{\mathcal{T}}^N \boldsymbol{\Psi}]_k \ge \boldsymbol{0}$ for $k = 1, \dots, N$, we get $\boldsymbol{\Psi}_k \ge \boldsymbol{0}$ for $k = 0, \dots, N$. □

**Theorem 3.1.** *Let $\boldsymbol{y}$ be the solution of (3.1a)–(3.1b) and $\boldsymbol{Y}$ be the solution of (3.20a)–(3.20b). Then we have the following a priori error estimate*

$$\|\boldsymbol{y}-\boldsymbol{Y}\|_{\overline{\Omega}^N} \leq C\vartheta(\Omega^N), \tag{3.25}$$

*where* $\vartheta(\Omega^N) := \max\limits_{1\leq k\leq N} \int\limits_{x_{k-1}}^{x_k} \left(1+\sum\limits_{m=1}^{\ell} \epsilon_m^{-1} \exp\left(-\frac{\beta s}{\epsilon_m}\right)\right) ds.$

**Proof.** From (3.24), we can get

$$\begin{aligned}
|\chi_i(x_k)| &\leq \epsilon_i \left|\left(D^- y_i(x) - \frac{d}{dx} y_i(x)\right)\Big|_{x=x_k}\right| + \left|\sum_{m=1}^{i-1} \tilde{\mathcal{R}}_{i,m}(x_k) \int_{x_{k-\varrho}}^{x_k} y_m'(s)\, ds\right| \\
&\quad + \left|\sum_{m=i+1}^{\ell} \tilde{\mathcal{R}}_{i,m}(x_k) \int_{x_{k-1}}^{x_k} y_m'(s)\, ds\right| \\
&\leq \epsilon_i \int_{x_{k-1}}^{x_k} |y_i''(s)|\, ds + C \int_{x_{k-\varrho}}^{x_k} \sum_{m=1}^{i-1} |y_m'(s)|\, ds + C \int_{x_{k-1}}^{x_k} \sum_{m=i+1}^{\ell} |y_m'(s)|\, ds \\
&\leq C \int_{x_{k-1}}^{x_k} \left(1+\sum_{n=1}^{\ell} \epsilon_m^{-1} \exp\left(-\frac{\beta s}{\epsilon_m}\right)\right) ds.
\end{aligned}$$

Consequently, we obtain $\|\boldsymbol{y}-\boldsymbol{Y}\|_{\overline{\Omega}^N} \leq C\vartheta(\Omega^N)$, which is the required result. □

Finally, we provide the following uniform convergence theorem for the proposed scheme on the a priori meshes, which may be proved along the same lines as previously discussed in Subsection 2.2.

**Theorem 3.2.** *Assuming $\boldsymbol{y}$ as the solution of (3.1a)–(3.1b) and $\boldsymbol{Y}$ as the approximate solution of (3.20a)–(3.20b), the following convergence result holds true*

$$\|\boldsymbol{y}-\boldsymbol{Y}\|_{\overline{\Omega}^N} \leq \begin{cases} CN^{-1}\ln N, & \text{(on Shishkin mesh)} \\ CN^{-1}, & \text{(on Bakhvalov mesh).} \end{cases}$$

### 3.4. A posteriori error analysis

In this subsection, we deduce the a posteriori error estimates corresponding to the nonlinear discrete problem (3.20a)–(3.20b). For the simplicity in further calculations, we denote $q_i(x) := b_i(x, \widetilde{\boldsymbol{Y}}(x));\ i=1,\ldots,\ell$. On the discretization mesh $\overline{\Omega}^N$, we consider the piecewise linear interpolants $\widetilde{Y}_i(x)$ & $\widetilde{q}_i(x)$ corresponding to $Y_{i,k}$ & $q_i$ $(k=1,\ldots,N)$, respectively. Clearly, $\widetilde{Y}_i(x)$ & $\widetilde{q}_i(x)$ are continuous on $\overline{\Omega}$, linear on each sub-intervals $[x_{k-1}, x_k]$ and defined by the following expressions

$$\begin{aligned}
\widetilde{Y}_i(x) &= Y_{i,k} + (x-x_k) D^- Y_{i,k}, \\
\widetilde{q}_i(x) &= q_{i,k} + (x-x_k) D^- q_{i,k}.
\end{aligned}$$

The above equations imply that it holds

$$\begin{aligned}
\widetilde{Y}_i(x_k) &= Y_{i,k}, \qquad \widetilde{q}_i(x_k) = q_{i,k}, \\
\left[\widetilde{Y}_i(x)\right]' &= D^- Y_{i,k}, \qquad \left[\widetilde{q}_i(x)\right]' = D^- q_{i,k}.
\end{aligned}$$

Further, we define the quantities that will be used in the next theorem. For Scheme I, we define $\hat{\mathcal{R}}_{i,m}(x_k) = \hat{a}_{i,m}(x_k)$ with

$$\hat{a}_{i,m}(x_k) = \frac{\partial b_i}{\partial u_m}\Big(x_k, \hat{v}_{1,k}, \ldots, \hat{v}_{i-1,k}, Y_{i,k}, \hat{v}_{i+1,k}, \ldots, \hat{v}_{\ell,k}\Big),$$

where $\hat{v}_{m,k}$ are the intermediate values, while for Scheme II, define $\hat{\mathcal{R}}_{i,m}(x_k) = 0, m=1,\ldots,i-1$, and $\hat{\mathcal{R}}_{i,m}(x_k) = \hat{a}_{i,m}(x_k)$ with

$$\hat{a}_{i,m}(x_k) = \frac{\partial b_i}{\partial u_m}\Big(x_k, Y_{1,k}, \ldots, Y_{i-1,k}, Y_{i,k}, \hat{v}_{i+1,k}, \ldots, \hat{v}_{\ell,k}\Big),$$

where $\hat{v}_{m,k}$ are the intermediate values.

Also, we define+

$$C_{3;i,m} = \max_{x,\boldsymbol{y}} |\hat{\mathcal{R}}_{i,m}|, \quad C_{4;i} = \max_{x,\boldsymbol{y}} \left|\frac{\partial^2 b_i(x,\boldsymbol{y})}{\partial x^2}\right|, \quad C_{5;i} = \max_{x,\boldsymbol{y},s} \left|\frac{\partial^2 b_i(x,\boldsymbol{y})}{\partial x\, \partial y_s(x)}\right|, \quad C_{6;i} = \max_{x,\boldsymbol{y},s,r} \left|\frac{\partial^2 b_i(x,\boldsymbol{y})}{\partial y_s(x)\, \partial y_r(x)}\right|.$$

**Theorem 3.3.** *Let $\mathbf{y}$ be the continuous solution of (3.1a)–(3.1b), $\mathbf{Y}$ be the discrete solution of (3.20a)–(3.20b). Assuming $\widetilde{\mathbf{Y}}$ as the piecewise linear interpolation of $\mathbf{Y}_k$, the following inequality holds*

$$\|\widetilde{\mathbf{Y}} - \mathbf{y}\|_\infty \leq C_2 \left(\tilde{\lambda}_1 + \tilde{\lambda}_2 + \tilde{\lambda}_3\right), \tag{3.26}$$

*where* $\tilde{\lambda}_j := \max\limits_{1\leq k\leq N} \tilde{\lambda}_{j,k}, j = 1,2,3$, *and*

$$\tilde{\lambda}_{1,k} := h_k \max_{1\leq i\leq \ell} \sum_{\substack{m=1\\ m\neq i}}^{\ell} C_{3;i,m} |D^- Y_{m,k}|, \qquad \tilde{\lambda}_{2,k} := h_k \max_{1\leq i\leq \ell} |D^- q_{i,k}|,$$

$$\tilde{\lambda}_{3,k} := \frac{h_k^2}{8} \max_{1\leq i\leq \ell} \left\{ C_{4;i} + C_{5;i} \sum_{s=1}^{\ell} |D^- Y_{s,k}| + C_{6;i} \left( \sum_{s=1}^{\ell} |D^- Y_{s,k}| \right)^2 \right\}.$$

**Proof.** For any $x \in (x_{k-1}, x_k)$, we have

$$\begin{aligned}
\mathcal{T}_i \widetilde{\mathbf{Y}}(x) - \mathcal{T}_i \mathbf{y}(x) &= \epsilon_i \left[\widetilde{Y}_i(x)\right]' + b_i(x, \widetilde{\mathbf{Y}}(x)) \\
&= \epsilon_i D^- Y_{i,k} + \widetilde{q}_i(x) + \left(q_i(x) - \widetilde{q}_i(x)\right) \\
&= \epsilon_i D^- Y_{i,k} + q_{i,k} + (x - x_k) D^- q_{i,k} + \left(q_i(x) - \widetilde{q}_i(x)\right) \\
&= -b_i(x_k, Y_1(x_{k-\varrho}), \ldots, Y_{i-1}(x_{k-\varrho}), Y_i(x_k), Y_{i+1}(x_{k-1}), \ldots, Y_l(x_{k-1})) \\
&\quad + b_i(x_k, Y_1(x_k), \ldots, Y_{\ell,k}) + (x - x_k) D^- q_{i,k} + \left(q_i(x) - \widetilde{q}_i(x)\right) \\
&= \sum_{m=1}^{i-1} \hat{\mathcal{R}}_{i,m}(x_k)(Y_{m,k} - Y_{m,k-\varrho}) + \sum_{m=i+1}^{\ell} \hat{\mathcal{R}}_{i,m}(x_k)(Y_{m,k} - Y_{m,k-1}) + (x - x_k) D^- q_{i,k} \\
&\qquad + \left(q_i(x) - \widetilde{q}_i(x)\right),
\end{aligned} \tag{3.27}$$

where (3.1a) and (3.23) are also used.

Now, we proceed as follows to evaluate each term of (3.27) one by one. First, we have

$$\begin{aligned}
\Big| \sum_{m=1}^{i-1} \hat{\mathcal{R}}_{i,m}(x_k)(Y_{m,k} - Y_{m,k-\varrho}) + \sum_{m=i+1}^{\ell} \hat{\mathcal{R}}_{i,m}(x_k)(Y_{m,k} - Y_{m,k-1}) \Big| &\leq \Big| \sum_{\substack{m=1\\ m\neq i}}^{\ell} \hat{\mathcal{R}}_{i,m}(x_k) h_k D^- Y_{m,k} \Big| \\
&\leq h_k \sum_{\substack{m=1\\ m\neq i}}^{\ell} C_{3;i,m} |D^- Y_{m,k}|.
\end{aligned} \tag{3.28}$$

Next, it holds

$$|(x - x_k) D^- q_{i,k}| \leq h_k |D^- q_{i,k}|. \tag{3.29}$$

Following to [32], it is straightforward to see that the function $q_i(x)$ satisfies

$$\|q_i(x) - \widetilde{q}_i(x)\|_\infty \leq \max_{1\leq k\leq N} \left\{ \frac{h_k^2}{8} \sup_{(x_{k-1}, x_k)} |q_i''(x)| \right\}.$$

Moreover, we have

$$\begin{aligned}
|q_i''(x)| &= \left| \frac{\partial^2 b_i(x, \widetilde{\mathbf{Y}}(x))}{\partial x^2} + \sum_{s=1}^{\ell} \frac{\partial^2 b_i(x, \widetilde{\mathbf{Y}}(x))}{\partial x\, \partial y_s(x)} \cdot \left(\widetilde{Y}_s(x)\right)' + \sum_{s=1}^{\ell} \sum_{r=1}^{\ell} \frac{\partial^2 b_i(x, \widetilde{\mathbf{Y}}(x))}{\partial y_s(x)\, \partial y_r(x)} \cdot \left(\widetilde{Y}_s(x)\right)' \cdot \left(\widetilde{Y}_r(x)\right)' \right| \\
&\leq C_{4;i} + C_{5;i} \sum_{s=1}^{\ell} \left| \left(\widetilde{Y}_s(x)\right)' \right| + C_{6;i} \sum_{s=1}^{\ell} \sum_{r=1}^{\ell} \left| \left(\widetilde{Y}_s(x)\right)' \right| \left| \left(\widetilde{Y}_r(x)\right)' \right| \\
&\leq C_{4;i} + C_{5;i} \sum_{s=1}^{\ell} \left| \left(\widetilde{Y}_s(x)\right)' \right| + C_{6;i} \left( \sum_{s=1}^{\ell} \left| \left(\widetilde{Y}_s(x)\right)' \right| \right)^2 \\
&\leq C_{4;i} + C_{5;i} \sum_{s=1}^{\ell} |D^- Y_{s,k}| + C_{6;i} \left( \sum_{s=1}^{\ell} |D^- Y_{s,k}| \right)^2.
\end{aligned}$$

Thus,

$$\|q_i(x)-\widetilde{q}_i(x)\|_{\infty}\leq \max_{1\leq k\leq N}\frac{h_k^2}{8}\left\{C_{4;i}+C_{5;i}\sum_{s=1}^{\ell}|D^{-}Y_{s,k}|+C_{6;i}\left(\sum_{s=1}^{\ell}|D^{-}Y_{s,k}|\right)^2\right\}. \tag{3.30}$$

Consequently, the required estimate (3.26) can be obtained by combining all these findings from (3.28)–(3.30) in (3.27) and using Corollary 3.1. □

## 4. Numerical experiments

In this section, we show the numerical results obtained for two different test problems, which corroborate in practice the theoretical conclusions established in this work. The numerical results are compared on a priori meshes as well as on a posteriori meshes. In this work, we generate the a posteriori meshes by following the mesh-generating algorithm originally proposed in [33]. For the convergence analysis of this algorithm in the singular perturbation context, one can see [22]. Many researchers have extensively used such algorithm for various classes of singularly perturbed problems (see [20,22,34–36], by instance).

As suggested in [22], we use the following relaxed or weakened form of the discrete equidistribution principle for any nonnegative monitor function $\boldsymbol{\Phi}$:

$$\boldsymbol{\Phi}_k\leq\frac{\rho}{N}\sum_{k=1}^{N}\boldsymbol{\Phi}_k,\quad k=1,\ldots,N, \tag{4.1}$$

where the constant $\rho>1$ is used to control the accuracy and iteration count.

### 4.1. Mesh generation algorithm

Step 1. Start with a uniform mesh $x_k^{(0)}=\{k/N,\ k=0,\ldots,N\}$, and set $r=0$.

Step 2. Calculate the discrete solution $Y_{i,k}^{(r)}$ on the mesh $x_k^{(r)}$ for linear and nonlinear problem separately, where $i=1,\ldots,\ell$ and $k=1,\ldots,N$.

Step 3. Calculate the subsequent discrete monitor functions:

$$\boldsymbol{\Phi}_k^{(r)}=\lambda_{1,k}+\lambda_{2,k}+\lambda_{3,k}+\lambda_{4,k}+\lambda_{5,k},\qquad\text{(for linear problem)}$$
$$\boldsymbol{\Phi}_k^{(r)}=\tilde{\lambda}_{1,k}+\tilde{\lambda}_{2,k}+\tilde{\lambda}_{3,k},\quad\text{(for nonlinear problem)}$$

for $k=1,\ldots,N$ and then compute $\Phi_m^{(r)}=\sum_{j=1}^{m}\boldsymbol{\Phi}_m^{(r)}$ for $m=1,\ldots,N$.

Step 4. **Stopping criterion:** if $\max_{1\leq k\leq N}\boldsymbol{\Phi}_k^{(r)}\leq\rho\frac{\Phi_N^{(r)}}{N}$ holds, proceed to Step 6, else move to the next step.

Step 5. Let $Q_k=k\frac{\Phi_N^{(r)}}{N}$ for $k=0,\ldots,N$. Construct new mesh $\{x_k^{(r+1)}\}$ by linear interpolation of the points $(\Phi_k^{(r)},x_k^{(r)})$ and evaluating at $Q_k$ for $k=0,1,\ldots,N$. Go to Step 2 with $r=r+1$.

Step 6. Consider $\{x_k^{(r)}\}$ as the ultimate adaptive mesh and $Y_{i,k}^{(r)}$ as the ultimate solution. **Stop**.

### 4.2. Numerical examples

Now, we will consider one test example for each linear and nonlinear type in the numerical experiment.

**Example 4.1** *([13]).* Consider a system of three linear equations of the form (2.1a)–(2.1b), where the coefficient matrices and vectors are given by

$$\mathcal{E}=\begin{pmatrix}\epsilon_1&0&0\\0&\epsilon_2&0\\0&0&\epsilon_3\end{pmatrix},\quad \mathcal{A}(x)=\begin{pmatrix}4&1&1\\-1&4+x&1\\2&-1&5+x\end{pmatrix},\quad \boldsymbol{g}(x)=\begin{pmatrix}x\\1\\1+x^2\end{pmatrix},\quad \boldsymbol{\gamma}=\begin{pmatrix}0\\0\\0\end{pmatrix}.$$

**Example 4.2.** Consider a system of three nonlinear equations of the form (3.1a)–(3.1b), where

$$\mathcal{E}=\begin{pmatrix}\epsilon_1&0&0\\0&\epsilon_2&0\\0&0&\epsilon_3\end{pmatrix},\ \boldsymbol{b}(x,\boldsymbol{y}(x))=\begin{pmatrix}3y_1(x)-\frac{1}{4}e^{-y_1^2(x)}-y_2(x)-y_3(x)-x^2+1\\-y_1(x)+4y_2(x)-\cos y_2(x)-y_3(x)-e^x\\-y_1(x)-y_2(x)+\sin y_3(x)+5y_3(x)-x\end{pmatrix},\ \boldsymbol{\gamma}^{\star}=\begin{pmatrix}0\\0\\0\end{pmatrix}.$$

To solve the nonlinear system of equations related to Example 4.2, Newton's method is applied with zero as the initial guess. The stopping criterion is defined as

**Table 1**
Uniform errors ($E^N$) and uniform convergence rates ($\rho^N$) for Example 4.1 obtained via splitting scheme (2.11).

| $N$ | Shishkin mesh | | Bakhvalov mesh | | A posteriori mesh | |
|---|---|---|---|---|---|---|
| | $E^N$ | $\rho^N$ | $E^N$ | $\rho^N$ | $E^N$ | $\rho^N$ |
| $2^6$ | 3.4938e-02 | 0.6911 | 1.0982e-02 | 0.9854 | 1.6631e-02 | 0.6402 |
| $2^7$ | 2.1641e-02 | 0.7528 | 5.5473e-03 | 0.9907 | 1.0671e-02 | 1.2864 |
| $2^8$ | 1.2843e-02 | 0.7973 | 2.7915e-03 | 0.9962 | 4.3748e-03 | 0.9860 |
| $2^9$ | 7.3900e-03 | 0.8289 | 1.3995e-03 | 0.9926 | 2.2087e-03 | 0.9982 |
| $2^{10}$ | 4.1602e-03 | 0.8517 | 7.0335e-04 | 0.9932 | 1.1057e-03 | 1.0009 |
| $2^{11}$ | 2.3054e-03 | 0.8684 | 3.5334e-04 | 1.0010 | 5.5251e-04 | 0.9954 |
| $2^{12}$ | 1.2628e-03 | 0.8812 | 1.7655e-04 | 0.9991 | 2.7715e-04 | 0.9999 |
| $2^{13}$ | 6.8559e-04 | – | 8.8330e-05 | – | 1.3858e-04 | – |

**Table 2**
Uniform errors ($E^N$) and uniform convergence rates ($\rho^N$) for Example 4.1 obtained via splitting scheme (2.12).

| $N$ | Shishkin mesh | | Bakhvalov mesh | | A posteriori mesh | |
|---|---|---|---|---|---|---|
| | $E^N$ | $\rho^N$ | $E^N$ | $\rho^N$ | $E^N$ | $\rho^N$ |
| $2^6$ | 2.4412e-02 | 0.5926 | 8.4223e-03 | 0.9739 | 4.8785e-03 | 1.0105 |
| $2^7$ | 1.6188e-02 | 0.6838 | 4.2878e-03 | 1.0206 | 2.4215e-03 | 1.1324 |
| $2^8$ | 1.0078e-02 | 0.7526 | 2.1135e-03 | 0.9239 | 1.1046e-03 | 0.9607 |
| $2^9$ | 5.9816e-03 | 0.8019 | 1.1139e-03 | 1.0382 | 5.6756e-04 | 1.0066 |
| $2^{10}$ | 3.4311e-03 | 0.8359 | 5.4243e-04 | 0.9658 | 2.8248e-04 | 0.9266 |
| $2^{11}$ | 1.9222e-03 | 0.8594 | 2.7773e-04 | 0.9512 | 1.4861e-04 | 1.0554 |
| $2^{12}$ | 1.0595e-03 | 0.8763 | 1.4364e-04 | 1.0198 | 7.1508e-05 | 0.9667 |
| $2^{13}$ | 5.7721e-04 | – | 7.0842e-05 | – | 3.6589e-05 | – |

$$\|\boldsymbol{Y}^{(n)} - \boldsymbol{Y}^{(n-1)}\|_{\infty} \leq 0.1 \times N^{-1}, \tag{4.2}$$

where $\boldsymbol{Y}^{(n)}$, for $n = 1, 2, \ldots$, represents the successive approximations to $\boldsymbol{Y}$ computed iteratively.

For the numerical experiments, we used the software MATLAB R2015a (The Mathworks, Inc.), on a 64-bit machine, with an Intel(R) Xeon(R) E5-2360 v4 processor running at 2.20 GHz and 64 GB RAM. Further, the perturbation parameters are chosen from the set $\mathcal{S}_\epsilon := \{(\epsilon_1, \epsilon_2, \epsilon_3) \mid \epsilon_3 = 2^0, 2^{-2}, \ldots, 2^{-20};\ \epsilon_2 = \epsilon_3, 2^{-2}\epsilon_3, \ldots, 2^{-26};\ \epsilon_1 = \epsilon_2, 2^{-2}\epsilon_2, \ldots, 2^{-30}\}$. A variant of the double-mesh principle has been utilized for the estimation of errors in the numerical solutions, as the exact solutions to the test examples are unknown. Thus, the errors are approximated by

$$E^N_{(\epsilon_1,\epsilon_2,\epsilon_3)} = \|\boldsymbol{Y}^N - \boldsymbol{Y}^{2N}\|_{\overline{\Omega}^N},$$

where $\boldsymbol{Y}^N$ represents the approximate solution obtained at $(N+1)$ mesh points, while $\boldsymbol{Y}^{2N}$ denotes the numerical solution on a mesh with $(2N+1)$ mesh points, obtained by bisecting the previous mesh; note that then, any interpolation is necessary. From the previous maximum errors, we calculate the uniform errors ($E^N$) and the corresponding numerical uniform convergence rates ($\rho^N$), in a usual way by

$$E^N = \max_{(\epsilon_1,\epsilon_2,\epsilon_3)\in\mathcal{S}_\epsilon} E^N_{(\epsilon_1,\epsilon_2,\epsilon_3)}, \quad \rho^N = \log_2\left(\frac{E^N}{E^{2N}}\right).$$

Tables 1 and 2 show the numerical results obtained on a priori meshes as well as a posteriori mesh for Example 4.1 using the discrete scheme (2.11)–(2.12), respectively. From them, we observe that both methods show uniform convergence of almost first order on the Shishkin mesh and first order for both the Bakhvalov and the a posteriori meshes. Moreover, the maximum errors are smallest for the Bakhvalov meshes when (2.11) is used and smallest for the a posteriori meshes when (2.12) is used.

Tables 3 and 4 show the numerical results computed on a priori meshes as well as a posteriori mesh for Example 4.2 using the discrete schemes (3.21) and (3.22), respectively. From them, we see again the same orders of uniform convergence as in the Example 4.1 and now the maximum errors are similar for both methods on the three meshes.

An important aspect of our algorithm, from a numerical point of view, is related with the number of iterations required to satisfy the stopping criterion (4.2); for fixed values of perturbation parameters and different values of $N$, this value is given in Tables 5 and 6 for splitting schemes (3.21) and (3.22), respectively. As we can see, the number of iterations is independent on the value of the discretization parameter $N$.

Tables 7 and 8 show a comparison of the computational time (*in seconds*) between our proposed schemes and existing standard discretization schemes, used to solve Examples 4.1 and 4.2, respectively. To calculate the computational times for Examples 4.1 and 4.2, we perform the experiments for all values of $\epsilon \in \mathcal{S}_\epsilon$ and taking $N = 2^6, \ldots, 2^{13}$. These tables clearly show that the proposed splitting schemes outperform the standard discretization schemes in terms of computational times. Moreover, the computational time

**Table 3**
Uniform errors ($E^N$) and uniform convergence rates ($\rho^N$) for Example 4.2 obtained via splitting scheme (3.21).

| $N$ | Shishkin mesh | | Bakhvalov mesh | | A posteriori mesh | |
|---|---|---|---|---|---|---|
| | $E^N$ | $\rho^N$ | $E^N$ | $\rho^N$ | $E^N$ | $\rho^N$ |
| $2^6$ | 3.1112e-02 | 0.6454 | 1.4589e-02 | 0.9607 | 1.4200e-02 | 0.9351 |
| $2^7$ | 1.9890e-02 | 0.7221 | 7.4961e-03 | 0.9801 | 7.4266e-03 | 1.0066 |
| $2^8$ | 1.2058e-02 | 0.7781 | 3.8000e-03 | 0.9900 | 3.6964e-03 | 0.9947 |
| $2^9$ | 7.0310e-03 | 0.8176 | 1.9132e-03 | 0.9949 | 1.8550e-03 | 1.0133 |
| $2^{10}$ | 3.9892e-03 | 0.8453 | 9.5995e-04 | 0.9975 | 9.1895e-04 | 0.9821 |
| $2^{11}$ | 2.2204e-03 | 0.8649 | 4.8081e-04 | 0.9987 | 4.6521e-04 | 1.0293 |
| $2^{12}$ | 1.2191e-03 | 0.8793 | 2.4062e-04 | 0.9994 | 2.2793e-04 | 0.9827 |
| $2^{13}$ | 6.6274e-04 | – | 1.2036e-04 | – | 1.1534e-04 | – |

**Table 4**
Uniform errors ($E^N$) and uniform convergence rates ($\rho^N$) for Example 4.2 obtained via splitting scheme (3.22).

| $N$ | Shishkin mesh | | Bakhvalov mesh | | A posteriori mesh | |
|---|---|---|---|---|---|---|
| | $E^N$ | $\rho^N$ | $E^N$ | $\rho^N$ | $E^N$ | $\rho^N$ |
| $2^6$ | 3.1095e-02 | 0.6449 | 1.1289e-02 | 0.9638 | 1.2363e-02 | 0.9517 |
| $2^7$ | 1.9887e-02 | 0.7219 | 5.7881e-03 | 0.9759 | 6.3922e-03 | 0.9497 |
| $2^8$ | 1.2057e-02 | 0.7781 | 2.9429e-03 | 0.9903 | 3.3095e-03 | 1.0292 |
| $2^9$ | 7.0309e-03 | 0.8176 | 1.4814e-03 | 0.9933 | 1.6216e-03 | 1.0035 |
| $2^{10}$ | 3.9893e-03 | 0.8453 | 7.4415e-04 | 0.9978 | 8.0879e-04 | 0.9918 |
| $2^{11}$ | 2.2204e-03 | 0.8649 | 3.7265e-04 | 0.9988 | 4.0671e-04 | 1.0288 |
| $2^{12}$ | 1.2191e-03 | 0.8793 | 1.8648e-04 | 0.9994 | 1.9934e-04 | 0.9483 |
| $2^{13}$ | 6.6274e-04 | – | 9.3280e-05 | – | 1.0331e-04 | – |

**Table 5**
Iteration counts for Example 4.2 obtained via splitting scheme (3.21) taking $\epsilon_3 = 2^{-6}, \epsilon_2 = 2^{-10}, \epsilon_1 = 2^{-14}$ and stopping criterion (4.2).

| | N | | | | | | | |
|---|---|---|---|---|---|---|---|---|
| Type of meshes ↓ | $2^6$ | $2^7$ | $2^8$ | $2^9$ | $2^{10}$ | $2^{11}$ | $2^{12}$ | $2^{13}$ |
| Shishkin meshes | 3 | 4 | 4 | 4 | 4 | 4 | 4 | 4 |
| Bakhvalov meshes | 3 | 4 | 4 | 4 | 4 | 4 | 4 | 4 |
| A posteriori meshes | 5 | 5 | 4 | 4 | 4 | 3 | 3 | 3 |

**Table 6**
Iteration counts for Example 4.2 obtained via splitting scheme (3.22) taking $\epsilon_3 = 2^{-6}, \epsilon_2 = 2^{-10}, \epsilon_1 = 2^{-14}$ and stopping criterion (4.2).

| | N | | | | | | | |
|---|---|---|---|---|---|---|---|---|
| Type of meshes ↓ | $2^6$ | $2^7$ | $2^8$ | $2^9$ | $2^{10}$ | $2^{11}$ | $2^{12}$ | $2^{13}$ |
| Shishkin meshes | 4 | 4 | 4 | 4 | 4 | 4 | 4 | 4 |
| Bakhvalov meshes | 4 | 4 | 4 | 4 | 4 | 4 | 4 | 4 |
| A posteriori meshes | 6 | 5 | 4 | 4 | 4 | 3 | 3 | 3 |

is bigger for the a posteriori mesh than for Shishkin or Bakhvalov meshes, as we expected, but the main advantage of our methods is that it requires a considerable smaller computational time than the classical backward Euler method; this difference increase notably in the case of the nonlinear system. So, we can conclude that our methods are more efficient than the classical methods used to solve the same type of problems.

Fig. 1a displays the numerical solution for Example 4.1, while Fig. 2a illustrates the numerical solution for Example 4.2. To enhance the visibility of the overlapping layer behavior near $x = 0$, we have included blow-up plots in Fig. 1b and Fig. 2b, respectively. In order to provide a clear visualization of convergence rates across different meshes, log-log plots are utilized, as depicted in Fig. 3. Furthermore, to illustrate the adaptive nature of the a posteriori mesh, we display the trajectory of mesh points at each iteration in Fig. 4. This figure clearly displays the condensation of mesh points towards the left side (near $x = 0$) and their subsequent adaptation to the solution behavior, thereby confirming the adaptivity of the a posteriori mesh. Note that, for the construction of plots in Figs. 3 and 4, we have used the splitting schemes (2.11) and (3.21) for Examples 4.1 and 4.2, respectively.

From a numerical point of view, an important question is the influence of the stopping criterion on the numerical results. Tables 9 to 11 show the results obtained for different values of the constant used in the stopping criterion for the Newton's method on the

**Table 7**
Comparison of computation time (in *seconds*) for Example 4.1 on various meshes.

| | Type of meshes | | |
|---|---|---|---|
| Scheme ↓ | Shishkin mesh | Bakhvalov mesh | A posteriori mesh |
| Splitting Scheme for $\mathcal{P} = \mathcal{P}_{\text{diag}}$, (2.11) | 132.7604 | 143.0740 | 663.3216 |
| Splitting Scheme for $\mathcal{P} = \mathcal{P}_{\text{ltr}}$, (2.12) | 131.0695 | 142.8700 | 660.9423 |
| Backward Euler Scheme ([13]) | 888.2355 | 890.3172 | 2231.0310 |

**Table 8**
Comparison of computation time (in *seconds*) for Example 4.2 on various meshes.

| | Type of meshes | | |
|---|---|---|---|
| Scheme ↓ | Shishkin mesh | Bakhvalov mesh | A posteriori mesh |
| Splitting Scheme (3.21) | 513.3180 | 523.0614 | 2080.5362 |
| Splitting Scheme (3.22) | 511.9097 | 520.6069 | 2081.7195 |
| Backward Euler Scheme ([17]) | 5133.1550 | 4317.1253 | 16034.5512 |

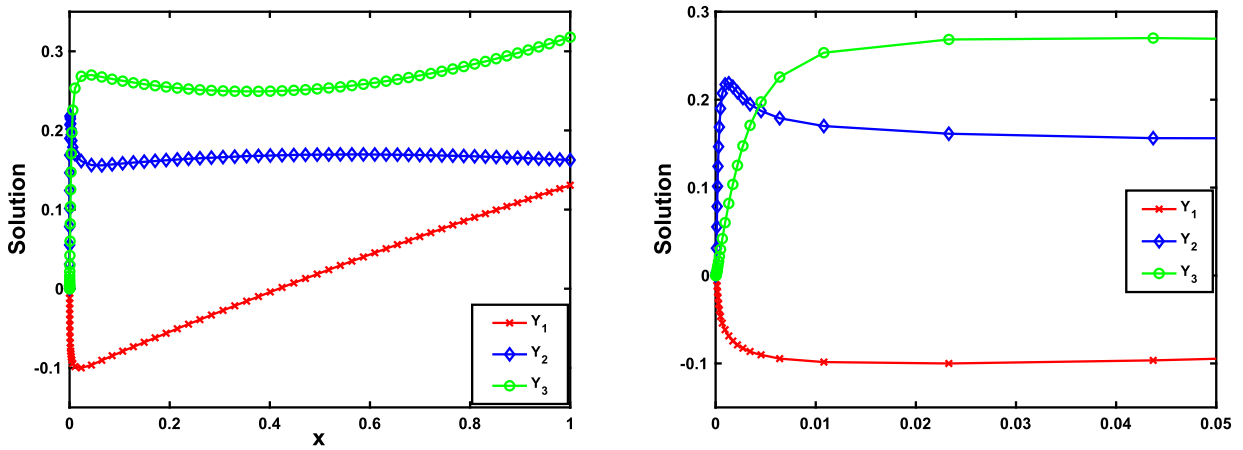


(a) Solution plot for Example 4.1 (b) Blow-up of the left figure in the sub-domain [0 0.05]

**Fig. 1.** Solution plots for Example 4.1 obtained via splitting scheme (2.11) for $\epsilon_1 = 2^{-14}$, $\epsilon_2 = 2^{-10}$, $\epsilon_3 = 2^{-6}$, and $N = 64$ using the a posteriori mesh.

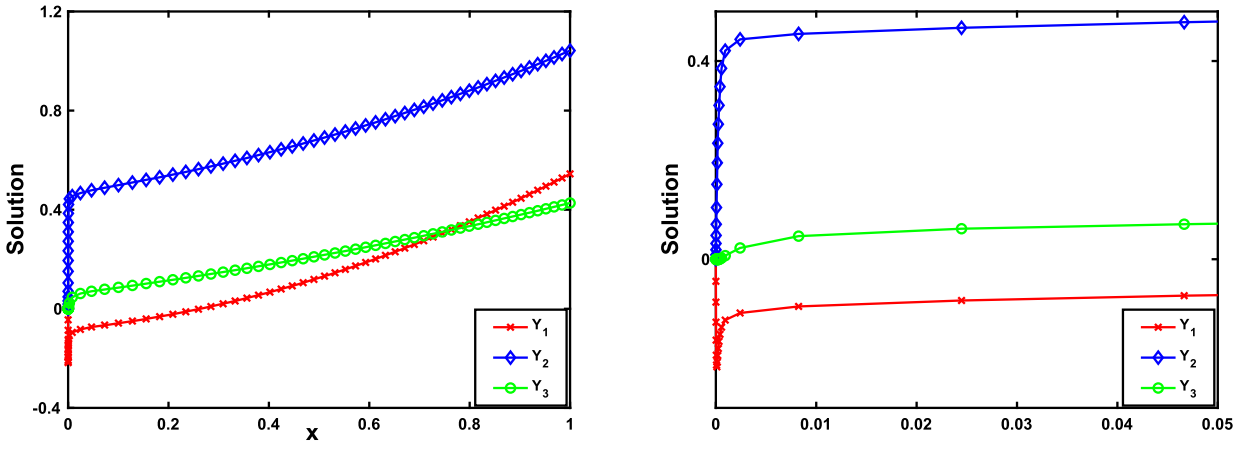


(a) Solution plot for Example 4.2 (b) Blow-up of the left figure in the sub-domain [0 0.05]

**Fig. 2.** Solution plots for Example 4.2 obtained via splitting scheme (3.21) for $\epsilon_1 = 2^{-14}$, $\epsilon_2 = 2^{-10}$, $\epsilon_3 = 2^{-6}$, and $N = 64$ using the a posteriori mesh.

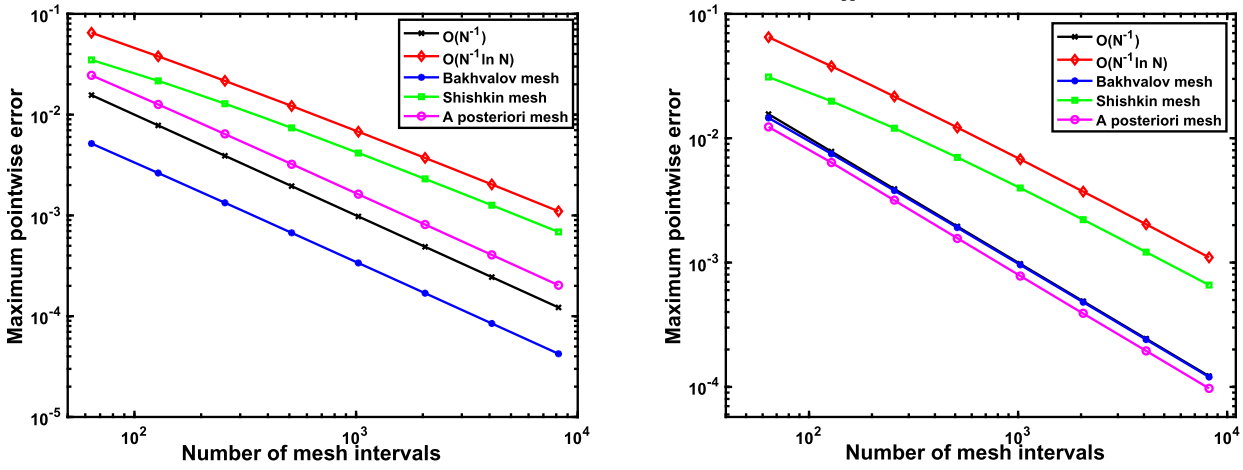


(a) Log-log plot for Example 4.1

(b) Log-log plot for Example 4.2

**Fig. 3.** Log-log plots of error vs. $N$ for $\epsilon_1 = 2^{-14}$, $\epsilon_2 = 2^{-10}$, $\epsilon_3 = 2^{-6}$ on various meshes.

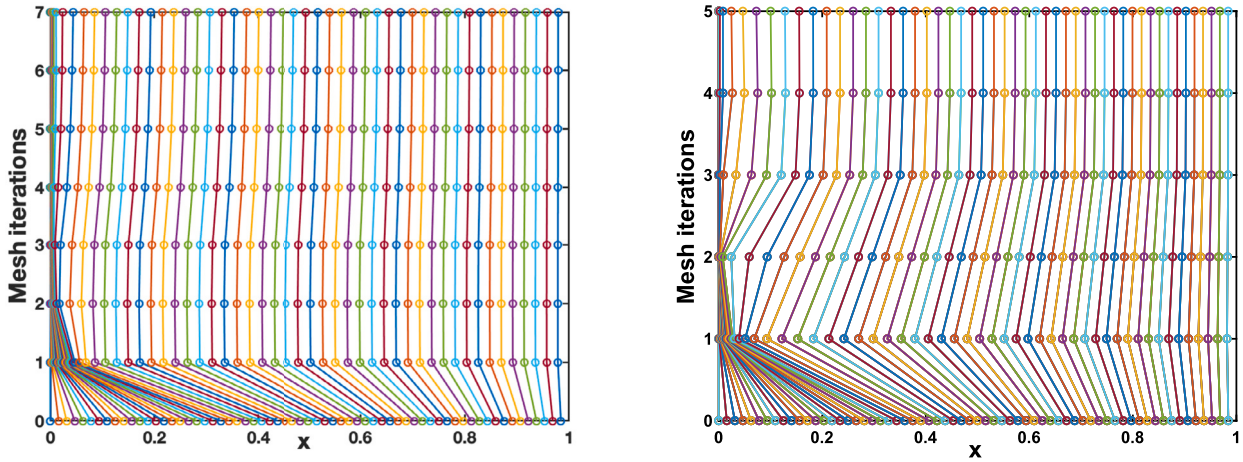


(a) Example 4.1

(b) Example 4.2

**Fig. 4.** Movement of a posteriori mesh points at each iteration for $\epsilon_1 = 2^{-14}$, $\epsilon_2 = 2^{-10}$, $\epsilon_3 = 2^{-6}$, and $N = 64$.

**Table 9**
Uniform errors ($E^N$) and uniform convergence rates ($\rho^N$) for Example 4.2 obtained via splitting scheme (3.21) on Shishkin mesh with different values of Tol.

| $N$ | Tol $= 0.1 \times N^{-1}$ | | Tol $= 0.01 \times N^{-1}$ | | Tol $= 10 \times N^{-1}$ | |
|---|---|---|---|---|---|---|
| | $E^N$ | $\rho^N$ | $E^N$ | $\rho^N$ | $E^N$ | $\rho^N$ |
| $2^6$ | 3.1112e-02 | 0.6454 | 3.1112e-02 | 0.6454 | 3.1111e-02 | 0.6453 |
| $2^7$ | 1.9890e-02 | 0.7221 | 1.9890e-02 | 0.7221 | 1.9890e-02 | 0.7221 |
| $2^8$ | 1.2058e-02 | 0.7781 | 1.2058e-02 | 0.7781 | 1.2058e-02 | 0.7781 |
| $2^9$ | 7.0310e-03 | 0.8176 | 7.0310e-03 | 0.8176 | 7.0310e-03 | 0.8176 |
| $2^{10}$ | 3.9892e-03 | 0.8453 | 3.9892e-03 | 0.8453 | 3.9892e-03 | 0.8453 |
| $2^{11}$ | 2.2204e-03 | 0.8649 | 2.2204e-03 | 0.8649 | 2.2204e-03 | 0.8649 |
| $2^{12}$ | 1.2191e-03 | 0.8793 | 1.2191e-03 | 0.8793 | 1.2191e-03 | 0.8793 |
| $2^{13}$ | 6.6274e-04 | – | 6.6274e-04 | – | 6.6274e-04 | – |

three different meshes when the diagonal splitting is used and Tables 12 to 14 when the lower triangular splitting is used; in all cases we see that there are not influence of the value of this constant on the numerical results.

Finally, Tables 15 and 16 show the number of iterations needed by algorithm by using different values of the constant used in the stopping criterion for the Newton's; again, in all cases we observe that it is not influential on the numerical results. Then, we can

**Table 10**
Uniform errors ($E^N$) and uniform convergence rates ($\rho^N$) for Example 4.2 obtained via splitting scheme (3.21) on Bakhvalov mesh with different values of Tol.

| $N$ | Tol $= 0.1 \times N^{-1}$ | | Tol $= 0.01 \times N^{-1}$ | | Tol $= 10 \times N^{-1}$ | |
|---|---|---|---|---|---|---|
| | $E^N$ | $\rho^N$ | $E^N$ | $\rho^N$ | $E^N$ | $\rho^N$ |
| $2^6$ | 1.4589e-02 | 0.9607 | 1.4589e-02 | 0.9607 | 1.4615e-02 | 0.9632 |
| $2^7$ | 7.4961e-03 | 0.9801 | 7.4961e-03 | 0.9801 | 7.4961e-03 | 0.9801 |
| $2^8$ | 3.8000e-03 | 0.9900 | 3.8000e-03 | 0.9900 | 3.8000e-03 | 0.9900 |
| $2^9$ | 1.9132e-03 | 0.9949 | 1.9132e-03 | 0.9949 | 1.9132e-03 | 0.9949 |
| $2^{10}$ | 9.5995e-04 | 0.9975 | 9.5995e-04 | 0.9975 | 9.5995e-04 | 0.9975 |
| $2^{11}$ | 4.8081e-04 | 0.9987 | 4.8081e-04 | 0.9987 | 4.8081e-04 | 0.9987 |
| $2^{12}$ | 2.4062e-04 | 0.9994 | 2.4062e-04 | 0.9994 | 2.4062e-04 | 0.9994 |
| $2^{13}$ | 1.2036e-04 | – | 1.2036e-04 | – | 1.2036e-04 | – |

**Table 11**
Uniform errors ($E^N$) and uniform convergence rates ($\rho^N$) for Example 4.2 obtained via splitting scheme (3.21) on a posteriori mesh with different values of Tol.

| $N$ | Tol $= 0.1 \times N^{-1}$ | | Tol $= 0.01 \times N^{-1}$ | | Tol $= 10 \times N^{-1}$ | |
|---|---|---|---|---|---|---|
| | $E^N$ | $\rho^N$ | $E^N$ | $\rho^N$ | $E^N$ | $\rho^N$ |
| $2^6$ | 1.4200e-02 | 0.9351 | 1.4200e-02 | 0.9351 | 1.4247e-02 | 0.9399 |
| $2^7$ | 7.4266e-03 | 1.0066 | 7.4266e-03 | 1.0066 | 7.4267e-03 | 1.0066 |
| $2^8$ | 3.6964e-03 | 0.9947 | 3.6964e-03 | 0.9947 | 3.6964e-03 | 0.9947 |
| $2^9$ | 1.8550e-03 | 1.0133 | 1.8550e-03 | 1.0133 | 1.8550e-03 | 1.0133 |
| $2^{10}$ | 9.1895e-04 | 0.9820 | 9.1895e-04 | 0.98209 | 9.1895e-04 | 0.9821 |
| $2^{11}$ | 4.6521e-04 | 1.0293 | 4.6521e-04 | 1.0293 | 4.6521e-04 | 1.0293 |
| $2^{12}$ | 2.2793e-04 | 0.9826 | 2.2793e-04 | 0.9827 | 2.2792e-04 | 0.9827 |
| $2^{13}$ | 1.1534e-04 | – | 1.1534e-04 | – | 1.1534e-04 | – |

**Table 12**
Uniform errors ($E^N$) and uniform convergence rates ($\rho^N$) for Example 4.2 obtained via splitting scheme (3.22) on Shishkin mesh with different values of Tol.

| $N$ | Tol $= 0.1 \times N^{-1}$ | | Tol $= 0.01 \times N^{-1}$ | | Tol $= 10 \times N^{-1}$ | |
|---|---|---|---|---|---|---|
| | $E^N$ | $\rho^N$ | $E^N$ | $\rho^N$ | $E^N$ | $\rho^N$ |
| $2^6$ | 3.1095e-02 | 0.6449 | 3.1095e-02 | 0.6449 | 3.1095e-02 | 0.6449 |
| $2^7$ | 1.9887e-02 | 0.7219 | 1.9887e-02 | 0.7219 | 1.9887e-02 | 0.7219 |
| $2^8$ | 1.2057e-02 | 0.7781 | 1.2057e-02 | 0.7781 | 1.2057e-02 | 0.7781 |
| $2^9$ | 7.0309e-03 | 0.8176 | 7.0309e-03 | 0.8176 | 7.0309e-03 | 0.8176 |
| $2^{10}$ | 3.9893e-03 | 0.8453 | 3.9893e-03 | 0.8453 | 3.9893e-03 | 0.8453 |
| $2^{11}$ | 2.2204e-03 | 0.8649 | 2.2204e-03 | 0.8649 | 2.2204e-03 | 0.8649 |
| $2^{12}$ | 1.2191e-03 | 0.8793 | 1.2191e-03 | 0.8793 | 1.2191e-03 | 0.8793 |
| $2^{13}$ | 6.6274e-04 | – | 6.6274e-04 | – | 6.6274e-04 | – |

**Table 13**
Uniform errors ($E^N$) and uniform convergence rates ($\rho^N$) for Example 4.2 obtained via splitting scheme (3.22) on Bakhvalov mesh with different values of Tol.

| $N$ | Tol $= 0.1 \times N^{-1}$ | | Tol $= 0.01 \times N^{-1}$ | | Tol $= 10 \times N^{-1}$ | |
|---|---|---|---|---|---|---|
| | $E^N$ | $\rho^N$ | $E^N$ | $\rho^N$ | $E^N$ | $\rho^N$ |
| $2^6$ | 1.1289e-02 | 0.9638 | 1.1289e-02 | 0.9638 | 1.1289e-02 | 0.9638 |
| $2^7$ | 5.7881e-03 | 0.9759 | 5.7881e-03 | 0.9759 | 5.7881e-03 | 0.9759 |
| $2^8$ | 2.9429e-03 | 0.9903 | 2.9429e-03 | 0.9903 | 2.9429e-03 | 0.9903 |
| $2^9$ | 1.4814e-03 | 0.9933 | 1.4814e-03 | 0.9933 | 1.4814e-03 | 0.9933 |
| $2^{10}$ | 7.4415e-04 | 0.9978 | 7.4415e-04 | 0.9977 | 7.4415e-04 | 0.9977 |
| $2^{11}$ | 3.7265e-04 | 0.9988 | 3.7265e-04 | 0.9988 | 3.7265e-04 | 0.9988 |
| $2^{12}$ | 1.8648e-04 | 0.9994 | 1.8648e-04 | 0.9994 | 1.8648e-04 | 0.9994 |
| $2^{13}$ | 9.3280e-05 | – | 9.3280e-05 | – | 9.3280e-05 | – |

**Table 14**
Uniform errors ($E^N$) and uniform convergence rates ($\rho^N$) for Example 4.2 obtained via splitting scheme (3.22) on a posteriori mesh with different values of Tol.

| $N$ | Tol $= 0.1 \times N^{-1}$ | | Tol $= 0.01 \times N^{-1}$ | | Tol $= 10 \times N^{-1}$ | |
|---|---|---|---|---|---|---|
| | $E^N$ | $\rho^N$ | $E^N$ | $\rho^N$ | $E^N$ | $\rho^N$ |
| $2^6$ | 1.2363e-02 | 0.9517 | 1.2363e-02 | 0.9517 | 1.2261e-02 | 0.9396 |
| $2^7$ | 6.3922e-03 | 0.9497 | 6.3922e-03 | 0.9497 | 6.3925e-03 | 0.9498 |
| $2^8$ | 3.3095e-03 | 1.0292 | 3.3095e-03 | 1.0292 | 3.3095e-03 | 1.0292 |
| $2^9$ | 1.6216e-03 | 1.0035 | 1.6216e-03 | 1.0035 | 1.6216e-03 | 1.0035 |
| $2^{10}$ | 8.0879e-04 | 0.9918 | 8.0879e-04 | 0.9918 | 8.0879e-04 | 0.9918 |
| $2^{11}$ | 4.0671e-04 | 1.0288 | 4.0671e-04 | 1.0288 | 4.0671e-04 | 1.0288 |
| $2^{12}$ | 1.9934e-04 | 0.9483 | 1.9934e-04 | 0.9483 | 1.9933e-04 | 0.9483 |
| $2^{13}$ | 1.0331e-04 | – | 1.0331e-04 | – | 1.0330e-04 | – |

**Table 15**
Iteration counts for Example 4.2 obtained via splitting scheme (3.21) taking $\epsilon_3 = 2^{-6}, \epsilon_2 = 2^{-10}, \epsilon_1 = 2^{-14}$ for different values of Tol.

| | | N | | | | | | | |
|---|---|---|---|---|---|---|---|---|---|
| Type of meshes ↓ | Tol ↓ | $2^6$ | $2^7$ | $2^8$ | $2^9$ | $2^{10}$ | $2^{11}$ | $2^{12}$ | $2^{13}$ |
| Shishkin meshes | $0.1 \times N^{-1}$ | 3 | 4 | 4 | 4 | 4 | 4 | 4 | 4 |
| | $0.01 \times N^{-1}$ | 4 | 4 | 4 | 4 | 4 | 4 | 4 | 4 |
| | $10 \times N^{-1}$ | 2 | 3 | 3 | 3 | 3 | 3 | 3 | 3 |
| Bakhvalov meshes | $0.1 \times N^{-1}$ | 3 | 4 | 4 | 4 | 4 | 4 | 4 | 4 |
| | $0.01 \times N^{-1}$ | 4 | 4 | 4 | 4 | 4 | 4 | 4 | 4 |
| | $10 \times N^{-1}$ | 2 | 3 | 3 | 3 | 3 | 3 | 3 | 3 |
| A posteriori meshes | $0.1 \times N^{-1}$ | 5 | 5 | 4 | 4 | 4 | 3 | 3 | 3 |
| | $0.01 \times N^{-1}$ | 5 | 5 | 4 | 4 | 4 | 3 | 3 | 3 |
| | $10 \times N^{-1}$ | 5 | 5 | 4 | 4 | 4 | 3 | 3 | 3 |

**Table 16**
Iteration counts for Example 4.2 obtained via splitting scheme (3.22) taking $\epsilon_3 = 2^{-6}, \epsilon_2 = 2^{-10}, \epsilon_1 = 2^{-14}$ for different values of Tol.

| | | N | | | | | | | |
|---|---|---|---|---|---|---|---|---|---|
| Type of meshes ↓ | Tol ↓ | $2^6$ | $2^7$ | $2^8$ | $2^9$ | $2^{10}$ | $2^{11}$ | $2^{12}$ | $2^{13}$ |
| Shishkin meshes | $0.1 \times N^{-1}$ | 4 | 4 | 4 | 4 | 4 | 4 | 4 | 4 |
| | $0.01 \times N^{-1}$ | 4 | 4 | 4 | 4 | 4 | 4 | 4 | 4 |
| | $10 \times N^{-1}$ | 2 | 3 | 3 | 3 | 3 | 3 | 3 | 3 |
| Bakhvalov meshes | $0.1 \times N^{-1}$ | 4 | 4 | 4 | 4 | 4 | 4 | 4 | 4 |
| | $0.01 \times N^{-1}$ | 4 | 4 | 4 | 4 | 4 | 4 | 4 | 4 |
| | $10 \times N^{-1}$ | 2 | 3 | 3 | 3 | 3 | 3 | 3 | 3 |
| A posteriori meshes | $0.1 \times N^{-1}$ | 6 | 5 | 4 | 4 | 4 | 3 | 3 | 3 |
| | $0.01 \times N^{-1}$ | 6 | 5 | 4 | 4 | 4 | 3 | 3 | 3 |
| | $10 \times N^{-1}$ | 6 | 5 | 4 | 4 | 4 | 3 | 3 | 3 |

conclude that our algorithm is an efficient method to solve the nonlinear coupled systems, which are considerably more difficult than the corresponding linear ones.

## 5. Conclusions

In this work, we have analyzed the numerical approximation of singularly perturbed initial value coupled systems of first-order, for which the diffusion parameters at each equation are distinct and they can have a different order of magnitude. We have considered both linear and nonlinear systems. For both types of problems, we have constructed efficient numerical methods which are defined on a priori meshes of Shishkin or Bakhvalov type and also on a posteriori meshes. In all cases, we have proved that the numerical method is uniformly convergent with respect to the diffusion parameter; moreover, it has almost first-order in the case of Shishkin mesh and first-order in the case of Bakhvalov and a posteriori meshes. We have shown the numerical results obtained for two different test problems without exact solution known; those results corroborate, in practice, the theoretical results and also the reduction of the computational cost in comparison with the classical backward Euler scheme; then, we can conclude that our algorithm is more efficient than the classical methods used to solve the same type of problems.

## CRediT authorship contribution statement

**Carmelo Clavero:** Writing – review & editing, Validation, Supervision, Methodology, Investigation, Formal analysis, Conceptualization. **Shashikant Kumar:** Writing – original draft, Software, Methodology, Investigation, Formal analysis, Conceptualization. **Sunil Kumar:** Writing – review & editing, Validation, Supervision, Methodology, Investigation, Formal analysis, Conceptualization.

## Funding

The research of the first author was partially supported by the project MTM2017-83490-P and the Aragón Government (European Social Fund (group E24-17R)). The third author was supported by the Science and Engineering Research Board, Government of India, through the Project No. CRG/2023/003228.

## Declaration of competing interest

The authors have no competing interests to declare that are relevant to the content of this article.

## Acknowledgements

The authors gratefully acknowledge the valuable comments and suggestions from the anonymous referees.

## References

[1] U.M. Ascher, R.M. Mattheij, R.D. Russell, Numerical Solution of Boundary Value Problems for Ordinary Differential Equations, Society for Industrial and Applied Mathematics, 1995.
[2] R.E. O'Malley, Singular Perturbation Methods for Ordinary Differential Equations, Springer, New York, 1991.
[3] J.J.H. Miller, E. O'Riordan, G.I. Shishkin, Fitted Numerical Methods for Singular Perturbation Problems: Error Estimates in the Maximum Norm for Linear Problems in One and Two Dimensions, World Scientific, Singapore, 1996.
[4] J.D. Murray, Mathematical Biology: I. An Introduction, Springer, New York, 2002.
[5] J. Banasiak, M. Lachowicz, Methods of Small Parameter in Mathematical Biology, Birkhäuser, Cham, 2014.
[6] A.C. Antoulas, Approximation of Large-Scale Dynamical Systems, Society for Industrial and Applied Mathematics, 2005.
[7] I. Raj, P.M. Johnson, J.J.H. Miller, V. Sigamani, A parameter uniform almost first order convergent numerical method for non-linear system of singularly perturbed differential equations, Biomath 5 (2) (2016) 1608111, https://doi.org/10.11145/j.biomath.2016.08.111.
[8] J.J.H. Miller, E. O'Riordan, Robust numerical method for a singularly perturbed problem arising in the modelling of enzyme kinetics, Biomath 9 (2) (2020) 2008227, https://doi.org/10.11145/j.biomath.2020.08.227.
[9] S. Hemavathi, T. Bhuvaneswari, S. Valarmathi, J.J.H. Miller, A parameter uniform numerical method for a system of singularly perturbed ordinary differential equations, Appl. Math. Comput. 191 (1) (2007) 1–11, https://doi.org/10.1016/j.amc.2006.05.218.
[10] S. Valarmathi, J.J.H. Miller, A parameter-uniform finite difference method for singularly perturbed linear dynamical systems, Int. J. Numer. Anal. Model. 7 (3) (2010) 535–548.
[11] P.M. Meenakshi, S. Valarmathi, J.J.H. Miller, Solving a partially singularly perturbed initial value problem on Shishkin meshes, Appl. Math. Comput. 215 (2010) 3170–3180, https://doi.org/10.1016/j.amc.2009.09.038.
[12] S.C.S. Rao, S. Kumar, Second order global uniformly convergent numerical method for a coupled system of singularly perturbed initial value problems, Appl. Math. Comput. 219 (2012) 3740–3753, https://doi.org/10.1016/j.amc.2012.09.075.
[13] S. Kumar, M. Kumar, Parameter-robust numerical method for a system of singularly perturbed initial value problems, Numer. Algorithms 59 (2012) 185–195, https://doi.org/10.1007/s11075-011-9483-4.
[14] G.M. Amiraliyev, The convergence of a finite difference method on layer-adapted mesh for a singularly perturbed system, Appl. Math. Comput. 162 (2005) 1023–1034, https://doi.org/10.1016/j.amc.2004.01.015.
[15] Z. Cen, J. Chen, L. Xi, A second-order hybrid finite difference scheme for a system of coupled singularly perturbed initial value problems, Int. J. Nonlinear Sci. 8 (2009) 148–154.
[16] Z. Cen, A. Xu, A. Le, A second-order hybrid finite difference scheme for a system of singularly perturbed initial value problems, J. Comput. Appl. Math. 234 (2010) 3445–3457, https://doi.org/10.1016/j.cam.2010.05.006.
[17] S. Kumar, M. Kumar, Analysis of some numerical methods on layer adapted meshes for singularly perturbed quasilinear systems, Numer. Algorithms 71 (2016) 139–150, https://doi.org/10.1007/s11075-015-9989-2.
[18] D. Shakti, J. Mohapatra, Numerical simulation and convergence analysis for a system of nonlinear singularly perturbed differential equations arising in population dynamics, J. Differ. Equ. Appl. 24 (2018) 1185–1196, https://doi.org/10.1080/10236198.2018.1468891.
[19] L. Liu, C. Zhu, G. Long, Numerical analysis of a system of semilinear singularly perturbed first-order differential equations on an adaptive grid, Math. Methods Appl. Sci. 45 (2022) 2042–2057, https://doi.org/10.1002/mma.7904.
[20] Sumit, S. Kumar, S. Kumar, A high order convergent adaptive numerical method for singularly perturbed nonlinear systems, Comput. Appl. Math. 41 (2022), https://doi.org/10.1007/s40314-022-01788-4.
[21] L.-B. Liu, Y. Chen, An adaptive moving grid method for a system of singularly perturbed initial value problems, J. Comput. Appl. Math. 274 (2015) 11–22, https://doi.org/10.1016/j.cam.2014.06.022.
[22] N. Kopteva, M. Stynes, A robust adaptive method for a quasi-linear one-dimensional convection-diffusion problem, SIAM J. Numer. Anal. 39 (4) (2001) 1446–1467.
[23] N. Kopteva, Maximum norm a posteriori error estimates for a one-dimensional convection-diffusion problem, SIAM J. Numer. Anal. 39 (2) (2001) 423–441.
[24] C. Clavero, J.C. Jorge, An efficient and uniformly convergent scheme for one-dimensional parabolic singularly perturbed semilinear systems of reaction-diffusion type, Numer. Algorithms 85 (3) (2020) 1005–1027.
[25] C. Clavero, J.C. Jorge, A splitting uniformly convergent method for one-dimensional parabolic singularly perturbed convection-diffusion systems, Appl. Numer. Math. 183 (2023) 317–332.
[26] S. Kumar, H. Ramos, J. Singh, An efficient hybrid numerical method based on an additive scheme for solving coupled systems of singularly perturbed linear parabolic problems, Math. Methods Appl. Sci. (2022).
[27] P.N. Vabishchevich, Additive schemes for certain operator-differential equations, Comput. Math. Math. Phys. 50 (12) (2010) 2033–2043.

[28] T. Linß, Layer-Adapted Meshes for Reaction-Convection-Diffusion Problems, Springer, Berlin, 2009.
[29] J.L. Gracia, F.J. Lisbona, E. O'Riordan, A system of singularly perturbed reaction-diffusion equations, DCU School of Mathematical Sciences, 2007, Preprint MS-07-10.
[30] J.L. Gracia, F.J. Lisbona, M. Madaune-Tort, E. O'Riordan, A system of singularly perturbed semilinear equations, in: BAIL 2008-Boundary and Interior Layers, Springer, 2009, pp. 163–172.
[31] R.S. Varga, Matrix Iterative Analysis, Springer, Berlin, 1962.
[32] K.E. Atkinson, An Introduction to Numerical Analysis, John Wiley & Sons, United Kingdom, 2008.
[33] C. De Boor, Good approximation by splines with variable knots. II, in: Conference on the Numerical Solution of Differential Equations, Springer, 1974, pp. 12–20.
[34] P. Das, Comparison of a priori and a posteriori meshes for singularly perturbed nonlinear parameterized problems, J. Comput. Appl. Math. 290 (2015) 16–25.
[35] S. Kumar, S. Kumar, Sumit, A posteriori error estimation for quasilinear singularly perturbed problems with integral boundary condition, Numer. Algorithms 89 (2) (2022) 791–809.
[36] J. Huang, Z. Cen, A. Xu, L.-B. Liu, A posteriori error estimation for a singularly perturbed Volterra integro-differential equation, Numer. Algorithms 83 (2) (2020) 549–563.